PICK1 links KIBRA and AMPA receptor subunit GluA2 in coiled-coil-driven supramolecular complexes

Received for publication, November 8, 2023, and in revised form, February 24, 2025 Published, Papers in Press, March 10, 2025,
https://doi.org/10.1016/j.jbc.2025.108397

Xin Shao[1] **and Lenora Volk**[1,2,3,4,*]

From the [1]*Department of Neuroscience,* [2]*Neuroscience Graduate Program,* [3]*Department of Psychiatry, and* [4]*Peter O'Donnell Jr Brain Institute Investigator, UT Southwestern Medical Center, Dallas, Texas, USA*

Reviewed by members of the JBC Editorial Board. Edited by Roger Colbran

The human memory-associated protein KIBRA regulates synaptic plasticity and trafficking of α-amino-3-hydroxy-5-methyl-4-isoxazolepropionic acid (AMPA)-type glutamate receptors, and is implicated in multiple neuropsychiatric and cognitive disorders. How KIBRA forms complexes with and regulates AMPA receptors remains unclear. Here, we show that KIBRA does not interact directly with the AMPA receptor subunit GluA2, but that protein interacting with C kinase 1 (PICK1), a key regulator of AMPA receptor trafficking, can serve as a bridge between KIBRA and GluA2. In contrast, KIBRA can form a complex with GluA1 independent of PICK1. We identified structural determinants of KIBRA-PICK1-AMPAR complexes by investigating interactions and cellular expression patterns of different combinations of KIBRA and PICK1 domain mutants. We find that the PICK1 BAR domain, a coiled-coil structure, is sufficient for interaction with KIBRA, whereas mutation of the PICK1 BAR domain disrupts KIBRA-PICK1-GluA2 complex formation. In addition, KIBRA recruits PICK1 into large supramolecular complexes, a process which requires KIBRA coiled-coil domains. These findings reveal molecular mechanisms by which KIBRA can organize key synaptic signaling complexes.

The *KIBRA* gene (enriched in KIdney and BRAin) is associated with human memory performance (1–13), and *Kibra* disruption impairs learning and memory in rodents (14–17). *KIBRA* polymorphisms and gene expression are also associated with disorders of complex brain function including schizophrenia (18), autism spectrum disorder (19), and Tourette syndrome (20). KIBRA is a scaffolding protein enriched at excitatory synapses (14, 21), with a large proportion of the KIBRA interactome also implicated in neuropsychiatric disorders (18, 22–27). Additionally, decreased KIBRA protein expression in the brain correlates with tauopathy-related cognitive impairment in humans (28, 29).

The involvement of KIBRA in the mechanisms underlying learning and memory remains incompletely understood. However, KIBRA has been shown to regulate synaptic plasticity, a cellular correlate of memory (30, 31), in multiple model organisms (14–17, 32, 33). KIBRA is also necessary for experience-induced plasticity of *in vivo* hippocampal and cortical circuit dynamics (34). Moreover, multiple studies have demonstrated that KIBRA can regulate the trafficking and expression levels of α-amino-3-hydroxy-5-methyl-4-isoxazolepropionic acid (AMPA) receptors, ionotropic glutamate receptors primarily responsible for fast excitatory neurotransmission in the central nervous system (14, 15, 17). As AMPA receptor trafficking is a highly conserved expression mechanism underlying many forms of excitatory synaptic plasticity (35, 36), KIBRA's influence on AMPA receptor trafficking is hypothesized to underlie its regulatory function in synaptic plasticity. While the specific cellular and molecular mechanisms underlying KIBRA's regulation of AMPA receptor trafficking remain unclear, experimental evidence indicates that KIBRA can form a complex with native AMPA receptors and regulators of AMPA receptor trafficking including GRIP1, NSF, Sec8, and protein interacting with C kinase 1 (PICK1) *in vivo* (14). Heterologous expression studies indicate that PICK1 interacts with KIBRA (14). PICK1 interacts directly with the GluA2 subunit of AMPARs and regulates synaptic plasticity and memory (37–39). It is not known if KIBRA binds GluA2 directly or if PICK1 can serve as a bridge between KIBRA and GluA2. Additionally, the molecular determinants regulating PICK1-KIBRA interactions are unknown.

KIBRA is a scaffolding protein containing multiple protein-protein and protein-lipid interaction domains (40, 41): two N-terminal WW domains (protein-interaction domains that bind PPxY motifs and other proline-rich regions) (42–44), central and C-terminal coiled-coil domains (CC domains mediate homotypic or heterotypic association with other coiled coils and facilitate oligomerization) (45, 46), a C2-like domain (mediating lipid binding, likely in a Ca^{2+}-independent manner) (40, 47), a glutamate-rich region, an atypical PKC-binding region (αBR) and a C-terminal type III PDZ (Postsynaptic Density-95/Discs large/Zonula occludens-1) ligand (mediating interaction with proteins containing PDZ domains) (48, 49). WW domain/PPxY interactions are ubiquitous among members of the HIPPO signaling pathway, which plays a conserved role in regulating cell growth, division, and organ size (42–44). Interestingly, WW domain mutants that disrupt KIBRA interaction with HIPPO signaling molecules exhibit stronger interaction with synaptic and AMPAR regulatory protein complexes, and hippocampal

* For correspondence: Lenora Volk, lenora.volk@utsouthwestern.edu.

overexpression of these KIBRA WW-domain mutants improves memory (50, 51).

PICK1 is unusual in that it contains both a PDZ domain and a BAR (Bin/Amphiphysin/RVS) domain (52). PDZ domains support protein-protein interactions with proteins containing C-terminal PDZ ligands, while BAR domains bind lipids, sense/regulate membrane curvature, and are commonly found in proteins involved in membrane trafficking (52, 53). The PICK1 PDZ domain preferentially binds type I and II PDZ ligands, among which are the GluA2 and GluA3 AMPAR subunits (52, 54). PICK1 BAR domain function is required for membrane trafficking of AMPARs (55, 56). BAR domains are composed of alpha-helical bundles that can engage in coiled-coil interactions with other proteins, including the promotion of PICK1 dimerization (55, 57–61). Notably, the PICK1 PDZ and BAR domains can interact with each other, promoting a closed conformation that disrupts some BAR domain interactions. Binding a PDZ ligand (*e.g.* GluA2) facilitates membrane localization and shifts PICK1 to an open conformation, promoting BAR domain activation (57, 59, 62–64).

To gain insight into mechanisms by which KIBRA regulates AMPAR complexes, we investigated the molecular basis of PICK1-KIBRA interactions by introducing mutations within the major functional domains of KIBRA and PICK1. Investigation of protein interactions and cellular expression patterns of protein complexes revealed that KIBRA does not bind GluA2 directly and that PICK1 can serve as a bridge between KIBRA and GluA2. In contrast, exogenously-expressed KIBRA and GluA1 can interact in the absence of additional intermediaries, suggesting the presence of multiple mechanisms through which KIBRA can couple to AMPARs. Our data further indicate that the PICK1 BAR domain regulates interaction with KIBRA, and that multiple domains of KIBRA can interact with PICK1. Additionally, we show that KIBRA initiates coiled-coil domain-dependent formation of large, supramolecular clusters with PICK1.

Results

PICK1 mediates interaction between KIBRA and GluA2, whereas KIBRA interacts with GluA1 independent of PICK1

While KIBRA plays a crucial role in regulating AMPAR trafficking, activity-induced increases in AMPAR expression, and synaptic plasticity (14, 15, 17, 50), how KIBRA complexes with AMPARs remains an open question. KIBRA interacts with the AMPAR-regulatory protein PICK1, which binds the GluA2 subunit of AMPARs through PDZ domain (PICK1)/PDZ ligand (GluA2) interactions (37, 65). To test the hypothesis that PICK1 facilitates KIBRA-AMPAR complex formation, we performed Co-IP (Co-Immunoprecipitation) experiments in HEK293T cells transfected with mCherry-KIBRA, Myc-GluA2, and either mGFP or mGFP-PICK1. Following immunoprecipitation of mCherry-KIBRA, co-precipitated GluA2 was detected using a Myc antibody. We found that Myc-GluA2 was only detected in the presence of co-expressed mGFP-PICK1, but not with mGFP alone (Fig. 1, *A* and *B*), indicating that KIBRA does not directly interact with GluA2 and that PICK1 can serve as a bridge between KIBRA and GluA2. Previous work indicated that KIBRA can interact with exogenously expressed GluA1 C-terminal peptide (17). To determine if KIBRA can interact with full-length GluA1, we performed similar Co-IP experiments in HEK293T cells transfected with mCherry-KIBRA, Myc-GluA1, and either mGFP or mGFP-PICK1. Following immunoprecipitation of mCherry-KIBRA, co-precipitated GluA1 was detected using a Myc antibody. We found that Myc-GluA1 was detected in the presence of either co-expressed mGFP-PICK1 or mGFP (Fig. 1, *C* and *D*), indicating that KIBRA can interact with GluA1 in the absence of additional co-expressed GluA1-interacting proteins and that PICK1 does not influence the interaction between KIBRA and homomeric GluA1 AMPARs, as expected given that PICK1 does not interact with GluA1. These data suggest the existence of multiple subunit-specific mechanisms by which KIBRA can complex with AMPA receptors.

To further investigate the function of KIBRA in AMPAR complexes, we examined the expression pattern of GluA2 alone or co-expressed with PICK1 or KIBRA. Consistent with prior reports (14, 37, 65), PICK1 and GluA2 show diffuse cytoplasmic localization when expressed alone in heterologous mammalian cells but form co-localized clusters when expressed together (Fig. 2, *A*, *D*, and *F*). Similarly, imaging of wild-type (WT) mouse hippocampal neurons transfected with mCherry-PICK1 and mGFP-KIBRA shows PICK1 co-clustered with KIBRA in dendrites (Fig. 2*I*). While not exclusive, PICK1-KIBRA co-clusters overlap with immunostaining for the synaptic marker synaptophysin (Fig. 2*I*), consistent with prior work showing similar punctate synaptic staining of endogenous and tagged PICK1 (55, 66). In contrast to PICK1 or GluA2, KIBRA forms large clusters when expressed alone in HEK293T cells (Fig. 2*B*) (14). We observed no co-clustering between co-expressed KIBRA and GluA2 in the absence of PICK1 (Fig. 2*B*), consistent with results from our co-immunoprecipitation experiments indicating that KIBRA does not directly interact with GluA2.

KIBRA promotes co-clustering of PICK1 and modulates PICK1-GluA2 clustering

It is well established that PICK1 plays a crucial role in the trafficking of GluA2-containing AMPA receptors (57). PICK1 clusters GluA2 in heterologous mammalian cells (Fig. 2, *A*, *D*, and *F*) (37) and regulates AMPAR trafficking in neurons (38, 59, 62, 67, 68). Because KIBRA clusters PICK1 in heterologous mammalian cells (Fig. 2*C*, S1, S3, and S4) (14) and also regulates AMPAR trafficking in neurons (14, 17), we predicted that KIBRA, PICK1, and GluA2 would form overlapping tripartite clusters when co-expressed in heterologous mammalian cells. Surprisingly, while KIBRA and PICK1 still formed large overlapping clusters in the presence of GluA2, concentrations of GluA2 were not precisely localized with PICK1/KIBRA clusters (Fig. 2*C*). We observed rings of GluA2 concentration surrounding some PICK1/KIBRA clusters (Fig. 2, *C*, *E*, and *G*). Line scans though the center of PICK1/KIBRA clusters revealed that the precise spatial co-localization of GluA2 with PICK1 is

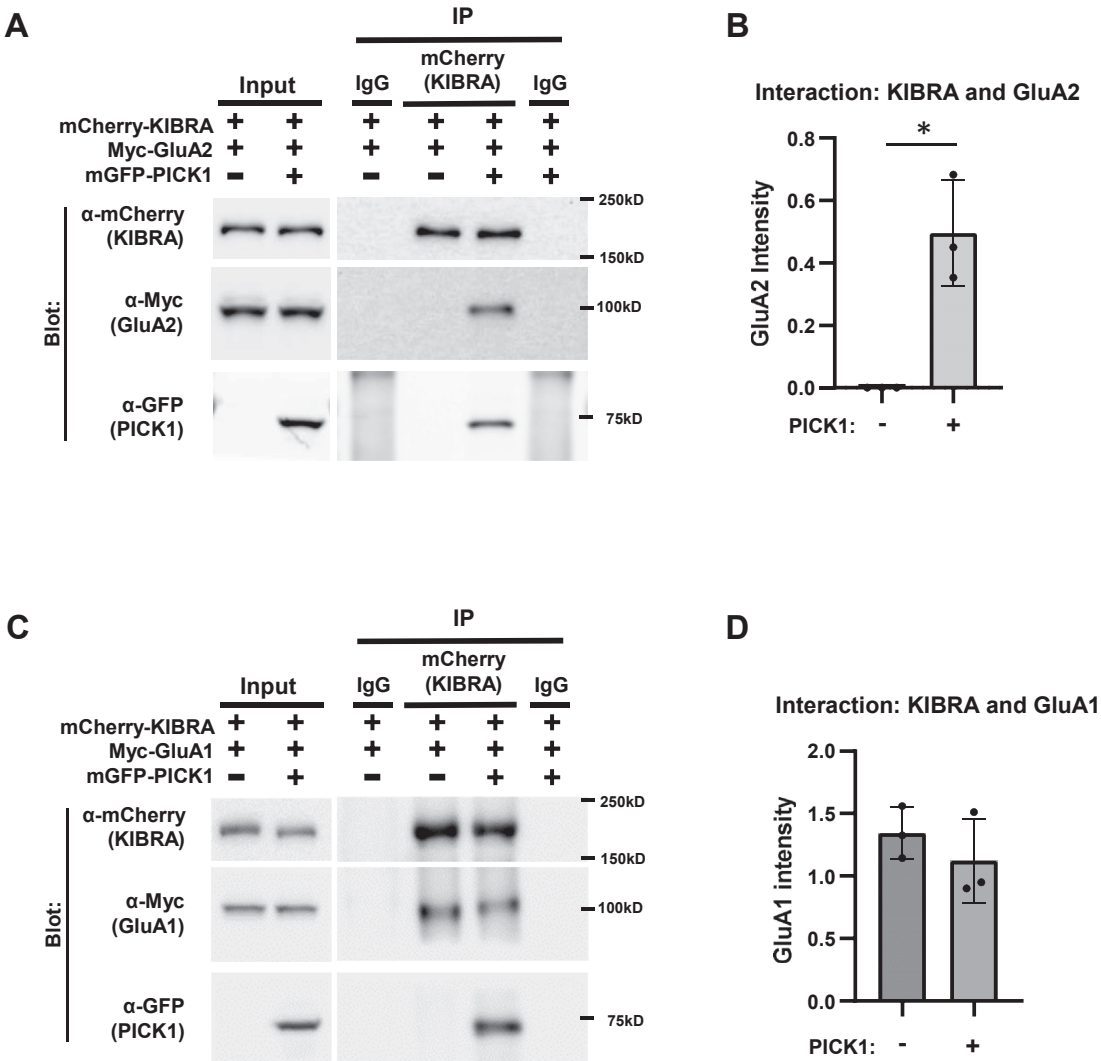

Figure 1. PICK1 mediates interaction between KIBRA and GluA2, while KIBRA interacts with GluA1 independently of PICK1. *A*, mCherry-KIBRA and Myc-GluA2 were transfected into HEK293T cells with either mGFP or mGFP-PICK1. mCherry antibody was used to immunoprecipitate mCherry-KIBRA, and co-precipitated Myc-GluA2 and mGFP-PICK1 were detected by immunoblot. *B*, quantification of three biological replicates showed that GluA2 was only coprecipitated with KIBRA in the presence of PICK1. GluA2 signal without PICK1: 0, with PICK1: 0.50 ± 0.17; n = 3; Paired, two-tailed *t* test, **p* = 0.0369. Data reported as mean ± SD. *C*, mCherry-KIBRA and Myc-GluA1 were transfected into HEK293T cells with either mGFP or mGFP-PICK1. mCherry antibody was used to immunoprecipitate mCherry-KIBRA, and co-precipitated Myc-GluA1 and mGFP-PICK1 were detected by immunoblot. *D*, quantification of three biological replicates showed that GluA1 was equally coprecipitated with KIBRA, regardless of the presence of PICK1. GluA1 signal without PICK1: 1.34 ± 0.21, with PICK1: 1.12 ± 0.34; n = 3; Paired, two-tailed *t* test, *p* = 0.5354. Data reported as mean ± SD.

altered by the presence of KIBRA (Fig. 2, *F–H*; GluA2 signal at the edge of PICK1/KIBRA clusters is significantly elevated compared to cellular background. Border mean ± SD = 107.3 ± 48.8, background = 71.6 ± 42.0, Wilcoxin test $p < 0.0001$, n = 70 cells from three biological replicates).

To determine if the redistribution of PICK1-GluA2 complexes in the presence of KIBRA results from altered PICK1-GluA2 interaction or altered PICK1 dimerization, we performed co-immunoprecipitations from HEK293T cells transfected with mGFP-PICK1, mCherry-PICK1, and Myc-GluA2 along with either Myc or Myc-KIBRA (Fig. 2, *J–L*). We find that KIBRA does not affect PICK1-GluA2 or PICK1-PICK1 interaction, suggesting that the reorganization of PICK1 and GluA2 by KIBRA is not due to altered interaction between PICK1 and GluA2 or disruption of PICK1 dimerization.

The BAR domain of PICK1 mediates co-clustering of PICK1 with KIBRA

PICK1 consists of two major functional domains: a BAR domain which facilitates PICK1 interaction with phospholipids and actin, and a PDZ domain responsible for interaction with proteins containing C-terminal PDZ ligands such as GluA2 (37, 55, 65). The cooperative action of the PDZ and BAR domains is vital for regulating AMPA receptor trafficking (57). Indeed, PICK1 BAR domain mutants impair the PICK1-dependent clustering of GluA2 in neurons and disrupt synaptic plasticity (55, 56). While PICK1 and KIBRA have been shown to interact in heterologous cells and *in vivo* (14), the nature of this interaction is unknown. To investigate the specific domains that regulate PICK1-KIBRA complex formation, we generated multiple PICK1 mutants that (1) disrupt PDZ domain interaction with proteins containing

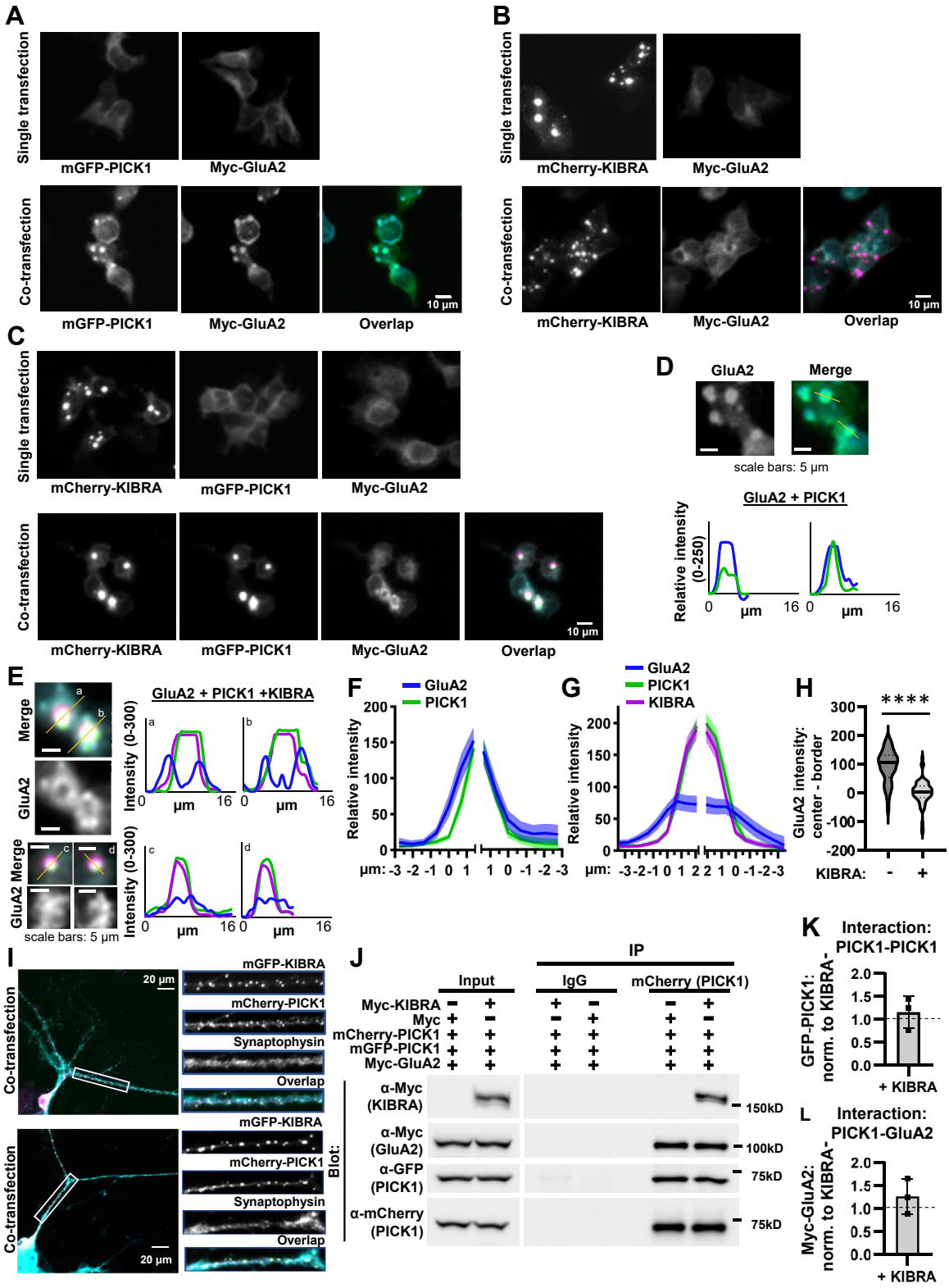

Figure 2. KIBRA promotes PICK1 cluster formation and alters PICK1/GluA2 co-clustering. *A*, mGFP-PICK1 and Myc-GluA2 were transfected into HEK293T cells. Singly transfected PICK1 and GluA2 show diffuse localization (*top*) whereas co-transfected PICK1 and GluA2 form clusters (*bottom*). *B*, mCherry-KIBRA and Myc-GluA2 were transfected into HEK293T cells. KIBRA forms puncta whether singly transfected (*top*) or co-transfected with GluA2 (bottom), but does not affect the diffuse localization of GluA2. *C*, mCherry-KIBRA, mGFP-PICK1 and Myc-GluA2 were transfected into HEK293T cells. Co-transfected KIBRA alters PICK1 and GluA2 co-clusters. *D*, example line scans of GluA2 and PICK1 in the indicated clusters from *panel A*. *E*, example line scans of GluA2, KIBRA, and PICK1 signals from the indicated clusters in *panel C*. *F* and *G*, summary of line scan quantification for HEK293T cells transfected with GluA2 and PICK1 (*F*) or GluA2, PICK1, and KIBRA (*G*). Data are plotted as mean ± 95% CI. Signals were aligned to the edges (x = 0) of each PICK1 (*F*) or KIBRA/PICK1 (*G*) cluster. *H*, GluA2 signal intensity at the border of each cluster was subtracted from the signal at the cluster center. *Dark lines* on the violin

PDZ ligands (KD-AA) (37, 69–74), (2) disrupt BAR domain interactions (5K-E) (55), or (3) truncate PICK1 to contain only the isolated BAR domain (Fig. 3*A*). Co-localized clustering between PICK1 and KIBRA was observed as expected upon transfection of mCherry-KIBRA WT and mGFP-PICK1 WT (Figs. 3*B* and S1, *A* and *B*) (14). The relative density of KIBRA puncta remained unchanged when co-expressed with PICK1 mutants or truncations (Fig. 3, *C–F*), consistent with data demonstrating that KIBRA can form clusters when expressed alone (Fig. 2, *B* and *C*) (14, 75). However, PICK1 clustering and the formation of PICK1-KIBRA co-clusters was reduced when KIBRA WT was co-transfected with the PICK1 BAR domain mutant (5K-E) (Fig. 3*C*), whereas co-transfection of KIBRA WT with the isolated PICK1 BAR domain still led to the formation of PICK1 co-clusters with KIBRA (Fig. 3*D*). Quantitative analysis showed that BAR domain mutation decreased the relative density of PICK1 clusters and the overlap between KIBRA and PICK1 puncta (Fig. 3, *G* and *H*). The isolated PICK1 BAR domain was more effective than WT PICK1 at promoting PICK1 clustering with KIBRA (Fig. 3, *H*), suggesting that the BAR domain is sufficient to mediate KIBRA-induced clustering of PICK1, and that other PICK1 domains may serve as regulatory elements influencing this interaction. While KIBRA does contain a PDZ ligand, it is a type III sequence, whereas PICK1 preferentially binds type I and II PDZ ligands, with a higher affinity for type II ligands (52). Additionally, the KIBRA fragment identified in the original yeast two-hybrid screen for PICK1 interactors did not contain the PDZ ligand (14). However, PICK1 BAR and PDZ domains can form intramolecular interactions, promoting a closed conformation that inhibits some intermolecular BAR-domain interactions (57, 59, 62, 63). Consistent with this model, we observe that disrupting PICK1 PDZ domain interactions (PICK1-KD-AA) also decreases KIBRA-induced PICK1 cluster formation and co-localization of PICK1 and KIBRA puncta (Fig. 3, *E*, *G*, and *H*).

To assess the impact of PICK1 domain mutants on KIBRA-PICK1-GluA2 clustering, we replicated the above experiments in the presence of GluA2, again finding that mutation of the PICK1 BAR or PDZ domain disrupts the ability of PICK1 to co-cluster with KIBRA (Fig. S1, *C*, *D*, *G*, and *H*), and the isolated PICK1 BAR domain is sufficient to cluster with KIBRA (Fig. S1, *E* and *F*). As expected, given that PICK1 binds GluA2 through its PDZ domain (37, 65) the isolated PICK1 BAR domain did not recruit GluA2 to the edges of PICK1-KIBRA clusters, and the PICK1 PDZ domain mutants that are released from KIBRA clusters fail to cluster GluA2 (Fig. S1, *G* and *H*).

We further validated the importance of the PICK1 BAR domain for KIBRA-induced PICK1 clustering in hippocampal neurons. We expressed PICK1 BAR domain mutants or isolated BAR domain in neurons cultured from PICK1 knockout mice to avoid confounds from endogenous WT PICK1 expression. At DIV10, neurons were transfected with mCherry-KIBRA WT and mGFP-PICK1 WT, 5K-E, or BAR, and imaging was conducted at DIV14. Consistent with the results obtained in HEK293T cells, PICK1 WT and isolated PICK1 BAR domain formed co-clusters with KIBRA WT in neurons (Fig. 3, *I*, *K*, *M*, and *N*). However, PICK1 5K-E BAR domain mutant protein failed to form co-clusters with KIBRA (Fig. 3, *J*, *M*, and *N*). The consistent results obtained in both neurons and HEK293T cells further support the notion that the BAR domain of PICK1 mediates its co-aggregation with KIBRA across various cell-types.

The PICK1 BAR domain regulates the interaction between PICK1 and KIBRA as well as the cohesion of the KIBRA-PICK1-GluA2 complex

Our data indicate that the PICK1 BAR domain is sufficient for PICK1 to cluster with KIBRA. The PICK1 BAR domain is a coiled-coil structure (Fig. 4*G*) that can mediate protein-protein in addition to protein-lipid interactions (55, 58–60, 62, 69, 76). Additionally, the PICK1 PDZ domain can influence BAR domain interactions (57, 59, 62, 63). We observe that mutation of the PDZ domain decreases PICK1-KIBRA clustering (Fig. 3). To determine if disrupted clustering reflects decreased PICK1-KIBRA interaction, we transfected mCherry-KIBRA along with mGFP-PICK1 WT, KD-AA, 5K-E, or BAR into HEK293T cells. Immunoprecipitation of mCherry-KIBRA was performed using an mCherry antibody, and the co-immunoprecipitated PICK1 was detected using a GFP antibody (Fig. 4*A*). The PICK1 BAR domain and PDZ domain mutants (5K-E, KD-AA) exhibited reduced interaction with KIBRA, while the isolated PICK1 BAR domain maintained strong interaction with KIBRA (Fig. 4*B*). These findings indicate that the PICK1 BAR domain is able to mediate PICK1 interaction with KIBRA. To determine whether KIBRA affects the interaction of PICK1 with other PICK1 BAR-binding proteins, we tested the interaction between PICK1 and dynamin (77). Our results indicate that the presence of KIBRA does not influence the binding of dynamin to PICK1 (Fig. S2), perhaps indicating that separate pools of PICK1 interact with KIBRA and dynamin (78).

As our data demonstrate that PICK1 mediates the interaction between KIBRA and GluA2, we sought to determine the role of PICK1 BAR domain interactions in the KIBRA-PICK1-

plot denote median, and dashed lines indicate quartiles. Mann-Whitney test, $p < 0.0001$; median and 95% CI limits: PICK1 +GluA2: = 106.3, 79.88 to 121.2, PICK1 + GluA2 + KIBRA = 2.447, −6.371 to 12.5. n = 36 cells for PICK1/GluA2-expressing cells and 70 cells for PICK1/GluA2/KIBRA-expressing cells, each from three biological replicates. Signals in *D–H* were measured following local background subtraction. *I*, mCherry-PICK1 and mGFP-KIBRA were transfected into wild-type (WT) mouse hippocampal neurons at DIV 10, and the neurons were subsequently immunostained for synaptophysin at DIV 14. Two representative neurons shown from independent cultures. Scale bars for *A–C* = 10 μm; scale bars for *D* and *E* = 5 μm; and scale bars for I = 20 μm. *J*, mGFP/mCherry-PICK1 and Myc-GluA2 were transfected into HEK293T cells with Myc or Myc-KIBRA. Anti-mCherry antibodies were used to immunoprecipitate mCherry-PICK1, and co-precipitated Myc-KIBRA, Myc-GluA2 and mGFP-PICK1 were detected by immunoblot using mGFP or Myc antibodies. *K* and *L*, PICK1 homodimerization (*K*, KIBRA+ normalized to KIBRA negative sample within the same gel: 1.15 ± 0.35; $p = 0.5287$) and PICK1-GluA2 interaction (*L*, KIBRA+, normalized to KIBRA-negative sample within the same gel: 1.26 ± 0.39; $p = 0.3594$) were not affected by KIBRA expression, quantified from three biological replicates. One sample *t* test *versus* 1. Data reported as mean ± SD unless otherwise noted.

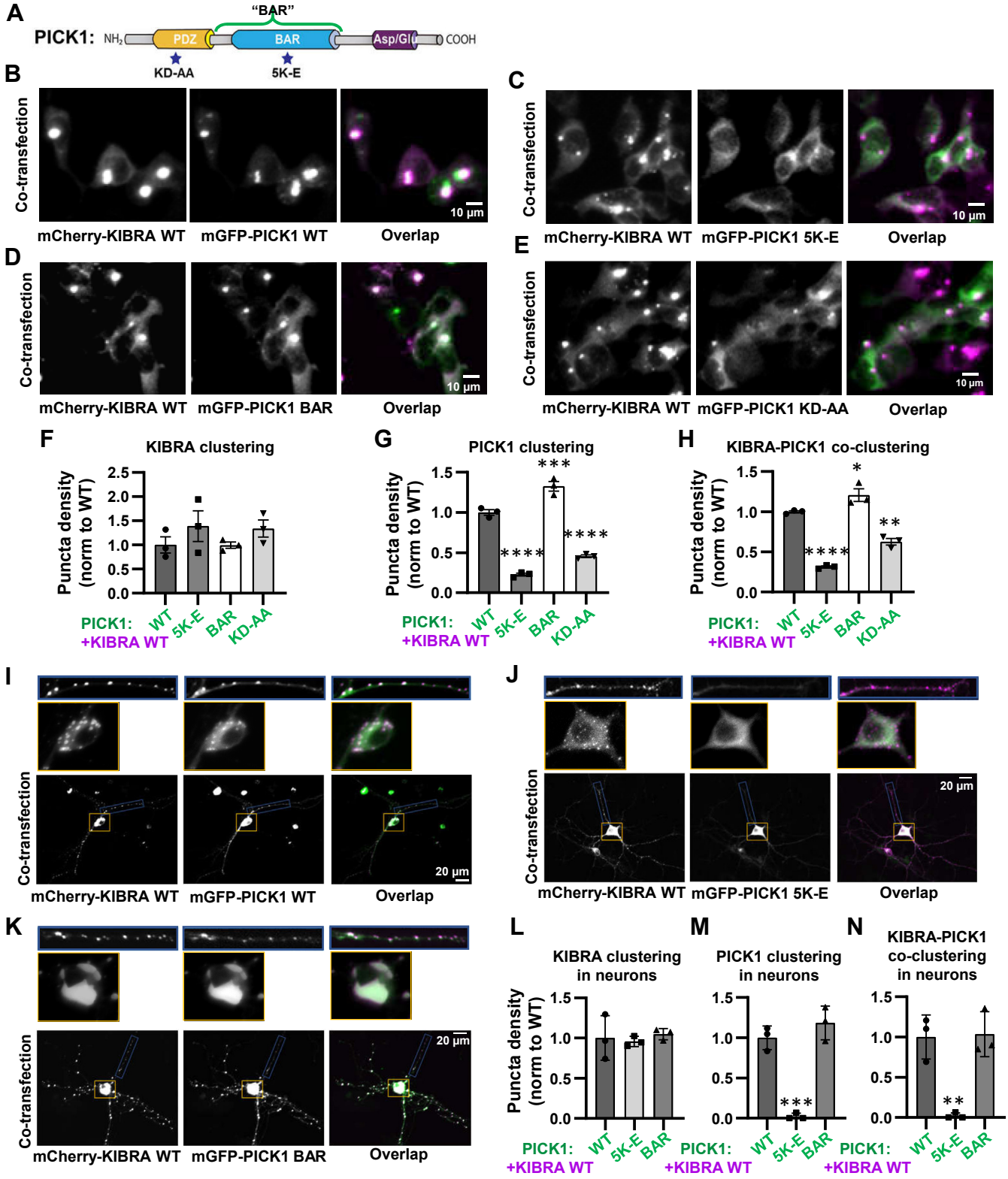

Figure 3. PICK1 BAR domain regulates the ability of PICK1 to co-cluster with KIBRA. *A*, PICK1 domain schematic with domain mutations. *B–E*, representative images of HEK-293T cells co-expressing KIBRA WT with (*B*) PICK1 WT, (*C*) PICK1 BAR domain mutant, 5K-E, (*D*) isolated PICK1 BAR domain, or (*E*) PICK1 PDZ-domain mutant, KD-AA. PICK1 WT and isolated BAR domain form clusters with KIBRA (*B* and *D*). Point mutants that disrupt BAR domain (5K-E) or PDZ domain (KD-AA) function result in diffuse PICK1 localization without affecting KIBRA clustering in HEK293T cells (*C* and *E*). *F–H*, quantification of three biological replicates from conditions shown in *B–E*; (*F*) Density of WT KIBRA puncta when co-expressed with PICK1 WT (1.00 ± 0.29), PICK1 5K-E (1.39 ± 0.55), PICK1 BAR (0.99 ± 0.11), PICK1 KD-AA (1.34 ± 0.31). Ordinary one-way ANOVA, F (3, 8) = 1.096, $p = 0.4051$, Dunnett's multiple comparisons test vs. WT; 5K-E $p = 0.4365$, BAR $p > 0.9999$, KD-AA $p = 0.5343$. *G*, density of PICK1 WT and mutant puncta when co-expressed with KIBRA WT; PICK1 WT (1.00 ± 0.05), PICK1 5K-E (0.23 ± 0.03), PICK1 BAR (1.33 ± 0.10), PICK1 KD-AA (0.46 ± 0.03). Ordinary one-way ANOVA, F (3, 8) = 192.6, $p < 0.0001$, Dunnett's multiple comparisons test vs. WT; 5K-E ****$p < 0.0001$, BAR ***$p = 0.0006$, KD-AA ****$p < 0.0001$. *H*, density of co-localized KIBRA WT and PICK1 WT (1.00 ± 0.02), PICK1 5K-E (0.31 ± 0.02), PICK1 BAR (1.21 ± 0.14), and PICK1 KD-AA (0.63 ± 0.07). Ordinary one-way ANOVA, F (3, 8) = 77.90, $p < 0.0001$, Dunnett's multiple comparisons

GluA2 complex. Consistent with prior work demonstrating PDZ domain/PDZ ligand-mediated interaction of PICK1 with GluA2 (37, 65), PICK1 BAR domain mutation (5K-E) does not disrupt the interaction between PICK1 and GluA2 (Fig. 4*C*). Subsequently, mGFP-PICK1 WT or 5K-E was co-transfected with Myc-GluA2 and mCherry-KIBRA WT into HEK293T cells to investigate how the PICK1 BAR domain mutation influences the KIBRA-PICK1-GluA2 complex (Fig 4*D*). As expected, the PICK1 5K-E mutation still disrupted PICK1-KIBRA interaction in the presence of GluA2 (Fig. 4*E*). Surprisingly, when KIBRA was present, the PICK1 5K-E mutation also disrupted PICK1 interaction with GluA2 (Fig. 4*F*). Consistent with these findings, PICK1 BAR domain mutants, which are released from KIBRA clusters, also fail to cluster GluA2 (Fig. S1, *C* and *D*). These data suggest that the presence of KIBRA can alter the nature of PICK1-GluA2 complex formation.

Coiled-coil domains mediate KIBRA-induced protein clustering

To assess the functional domains involved in KIBRA localization and cluster formation, we transfected HEK293T cells with mGFP-KIBRA WT or various KIBRA truncations: ΔWW, ΔCoiled-coil linker (ΔCCL), ΔC2, ΔC terminal (ΔCt), or ΔαBR (Fig. 5*A*) along with mCherry-PICK1 WT. As previously demonstrated, KIBRA WT formed large clusters, and PICK1 co-clustered with KIBRA WT (Fig. 5*B*, see also Figs. 2 and 3). Deletion of KIBRA's coiled-coil linker or the C-terminal region which also contains coiled-coil structure (see Fig. 6*E*) resulted in diffuse distribution of KIBRA and PICK1 (Fig. 5, *C* and *D*). Conversely, KIBRA ΔWW, ΔC2, and ΔαBR still retained the ability to form clusters, and PICK1 exhibited co-clustering with these truncations (Fig. S3). Quantification of ΔCCL or ΔCt truncations revealed a dramatic decrease in KIBRA puncta density (Fig. 5*E*). Both the relative PICK1 puncta density and the density of puncta co-expressing KIBRA and PICK1 also decreased substantially with KIBRA coiled-coil linker or C-terminal truncations (Fig. 5, *F* and *G*). Because the coiled-coil linker and C-terminal domain encompass the majority of KIBRA coiled-coil structure (Fig. 6*E*), our results suggest that the coiled-coil domains of KIBRA can mediate clustering of KIBRA and PICK1. To assess the impact of clustering-deficient KIBRA mutants on PICK1-GluA2 clustering, we repeated the above experiments in the presence of GluA2 (Fig. S4). As reported in Figure 5, KIBRA ΔCCL or ΔCt truncations show diffuse expression (Fig. S4, *C*–*F*). Notably, we observed co-clustering of PICK1 and GluA2 in KIBRA ΔCCL or ΔCt truncations, suggesting that large, supramolecular KIBRA complexes spatially sequester PICK1 from GluA2.

To test if the cluster-promoting role of KIBRA's coiled-coil-containing domains was conserved in neurons, we expressed KIBRA WT, ΔCCL, or ΔCt with PICK1 WT in hippocampal neurons. Cultured neurons were prepared from KIBRA knockout mice (14) to circumvent complications from endogenous WT KIBRA complexing with exogenously-expressed mutants. Consistent with the results in HEK293T cells, PICK1 WT formed co-clusters with KIBRA WT (Fig. 5*H*), whereas KIBRA ΔCCL, or ΔCt showed diffuse localization and failed to cluster PICK1 (Fig. 5, *I* and *J*). Quantification showed a dramatic decrease in relative KIBRA puncta density (Fig. 5*K*), PICK1 puncta density (Fig. 5*L*), and KIBRA-PICK1 co-clusters (Fig. 5*M*) with KIBRA ΔCCL, or ΔCt mutants. These similar results between cultured neurons and HEK293T cells indicate a consistent role for KIRBA coiled-coil domains in promoting KIBRA-PICK1 clustering across different cell types, including in neurons.

No single domain of KIBRA is responsible for mediating the interaction between KIBRA and PICK1

To identify the KIBRA domain(s) mediating interaction with PICK1, and to determine if the role of KIBRA coiled-coil-containing domains in promoting KIBRA-PICK1 clustering reflects coiled-coil-mediated protein interaction, we transfected HEK293T cells with KIBRA WT or domain deletions (ΔWW, Δcoiled-coil linker, ΔC2, ΔC-terminal, or ΔαBR) along with mCherry-PICK1 WT. PICK1 was immuno precipitated using a mCherry antibody, and the co-immunoprecipitated KIBRA was detected with a GFP antibody (Fig. 6*A*). Quantification of five biological replicates revealed that none of the KIBRA domain truncations disrupted interaction between KIBRA and PICK1 (Fig. 6*B*). In fact, WW domain deletion increased PICK1-KIBRA interaction (Fig. 6*B*), consistent with recent work demonstrating that mutation of KIBRA WW domains disrupts interaction with HIPPO signaling molecules, releasing KIBRA to increase its association with AMPA receptor complexes (50). Surprisingly, we also find that C-terminal KIBRA truncation enhances interaction with PICK1 (Fig. 6*B*). mCherry-PICK1 does not interact with GFP alone (Fig. S5*A*), indicating that PICK1-KIBRA interaction as measured by co-IP is not a nonspecific artifact of PICK1 interaction with GFP.

Multimerization plays an important role in the ability of scaffolding proteins to organize signaling complexes (75, 78–80). KIBRA can form homodimers (21, 81) and large multimolecular clusters (Figs. 2, 3, 5, S1, S3, and S4) (14, 75, 82).

test vs. WT; 5K-E ****$p < 0.0001$, BAR *$p = 0.0284$, KD-AA **$p = 0.0010$. *I–K*, WT KIBRA was expressed with PICK1 WT, PICK1 BAR domain mutant, or isolated PICK1 BAR domain in hippocampal neurons cultured from PICK1 KO mice. PICK1 WT and isolated BAR domain form clusters with KIBRA while PICK1 5K-E shows diffuse localization in both the cell body and dendrites. *L–N*, quantification of three biological replicates from conditions shown in (*I–K*). *L*, Density of WT KIBRA puncta in neurons when co-expressed with PICK1 WT (1.00 ± 0.28), PICK1 5K-E (0.96 ± 0.06), PICK1 BAR (1.05 ± 0.07). Ordinary one-way ANOVA, F (2, 6) = 0.2162, $p = 0.8116$, Dunnett's multiple comparisons test vs. WT; 5K-E $p = 0.9313$, BAR $p = 0.9192$. *M*, density of PICK1 WT and mutant puncta when co-expressed with KIBRA WT; PICK1 WT (1.00 ± 0.15), PICK1 5K-E (0.02 ± 0.04), PICK1 BAR (1.18 ± 0.21). Ordinary one-way ANOVA, F (2, 6) = 52.01, $p = 0.0002$, Dunnett's multiple comparisons test vs. WT; 5KE ***$p = 0.0004$, BAR $p = 0.2998$. *N*, density of KIBRA WT co-localized with PICK1 WT (1.00 ± 0.27), PICK1 5K-E (0.03 ± 0.02), or PICK1 BAR (1.04 ± 0.28). Ordinary one-way ANOVA, F (2, 6) = 19.34, $p = 0.0024$, Dunnett's multiple comparisons test vs. WT; 5K-E **$p = 0.0033$, BAR $p = 0.8748$. Data reported as mean ± SD. Scale bars in *B–E* = 10 μm. Scale bars for I–K = 20 μm. For quantification in *F–H* and *L–N*, all values were normalized to the average of the three WT biological replicates (independent cultures).

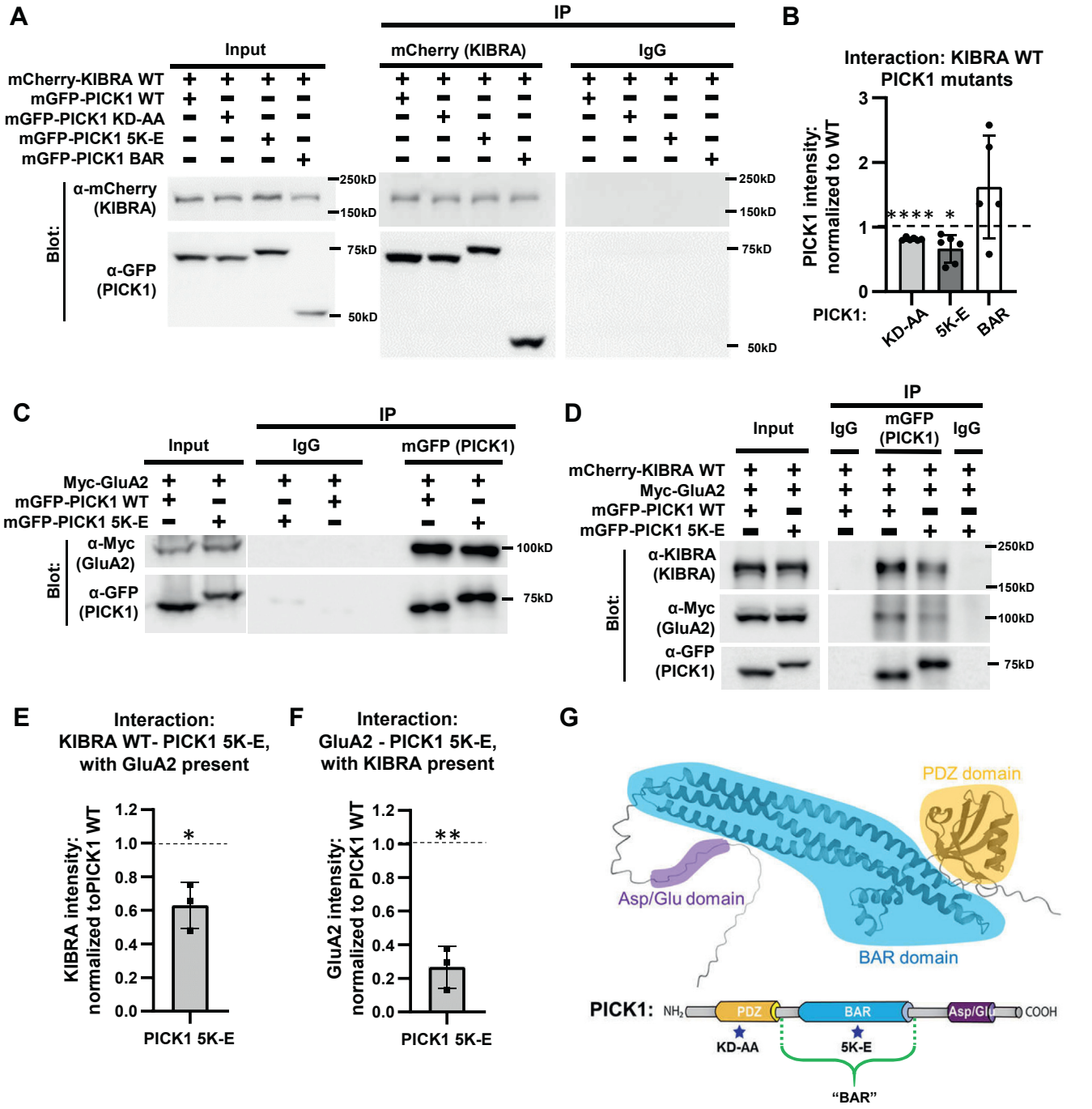

Figure 4. PICK1 BAR domain facilitates the interaction between KIBRA and PICK1. *A*, mGFP-PICK1 WT, KD-AA, 5K-E or BAR was transfected with mCherry-KIBRA WT into HEK293T cells. mCherry-KIBRA was immunoprecipitated and co-precipitated mGFP-PICK1 variants were detected by immunoblot using anti-GFP antibodies. *B*, quantification of six biological replicates for PICK1 WT, KD-AA and 5K-E and five biological replicates for PICK1 BAR as shown in *A*; PICK1 KD-AA or 5K-E impair interaction with KIBRA compared with PICK1 WT (PICK1 pull down normalized to input and same-gel WT PICK1; PICK1 KD-AA: 0.81 ± 0.02, ****$p < 0.0001$; PICK1 5K-E: 0.67 ± 0.21, *$p = 0.0127$; PICK1 BAR: 1.62 ± 0.79, $p = 0.1541$, one sample *t* test *versus* 1). *C*, mGFP-PICK1 WT or 5K-E and Myc-GluA2 were transfected into HEK293T cells. Immunoprecipitation of PICK1 was performed using a GFP antibody, and the co-precipitated GluA2 was detected using a Myc antibody. GluA2 showed equivalent interaction with mGFP-PICK1 WT and 5K-E. *D*, mGFP-PICK1 WT or 5K-E was co-transfected with mCherry-KIBRA and Myc-GluA2 into HEK293T cells. mGFP-PICK1 was immunoprecipitated and co-precipitated mCherry-KIBRA and Myc-GluA2 were detected by immunoblot. *E* and *F*, quantification of three biological replicates of conditions shown in *D*; When PICK1, KIBRA and GluA2 are all present, mutation of the PICK1 BAR domain (PICK1 5K-E) decreases interaction with both KIBRA and GluA2. (All bands were normalized to input. KIBRA signal with PICK1 5K-E normalized to +PICK1 WT: 0.63 ± 0.14, *$p = 0.0434$; GluA2 signal with PICK1 5K-E normalized to +PICK1 WT: 0.27 ± 0.13, **$p = 0.0096$, one sample *t* test.) *G*, structure and domains of PICK1. Predicted structure modified from AlphaFold Protein Structure Database. Data reported as mean ± SD.

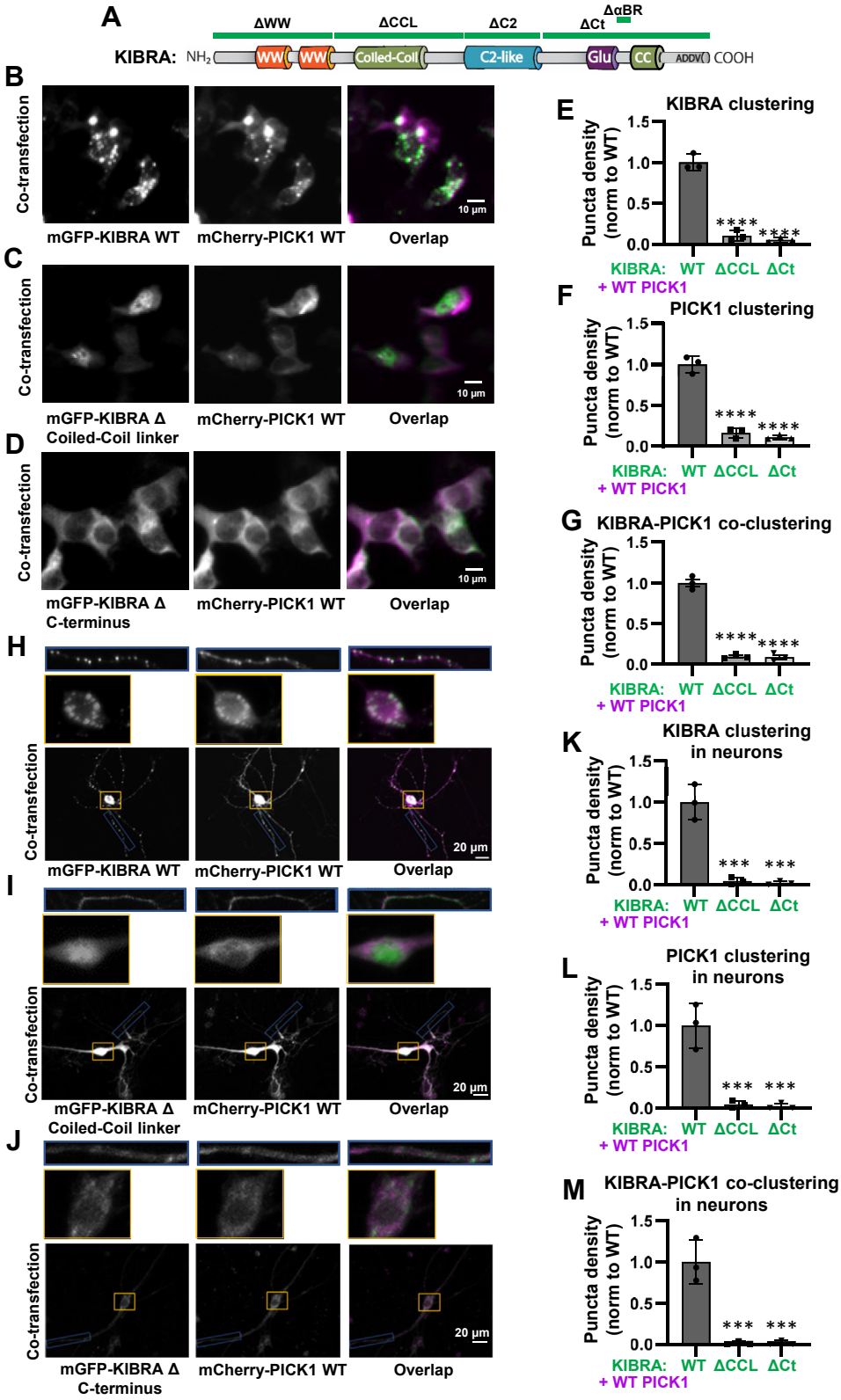

Figure 5. KIBRA coiled-coil-containing domains contribute to KIBRA clustering and subsequent PICK1 co-clustering. *A*, KIBRA domain schematic with the location of domain truncations noted. *B–D*, KIBRA WT clusters with PICK1 WT while KIBRA mutants missing the coiled-coil linker or C-terminal regions (ΔCCL and ΔCt, respectively) show diffuse localization and fail to cluster PICK1 in HEK293T cells. *E–G*, quantification of three biological replicates for conditions shown in *B–D*. *E*, KIBRA puncta density for KIBRA WT (1.00 ± 0.10), KIRBA ΔCCL (0.10 ± 0.07), and KIBRA ΔCt (0.05 ± 0.03). Ordinary one-way ANOVA, F (2, 6) = 170.8, $p < 0.0001$, Dunnett's multiple comparisons test vs. WT, KIRBA ΔCCL and ΔCt ****$p < 0.0001$. *F*, PICK1 cluster density when co-expressed with KIBRA WT (1.00 ± 0.10), ΔCCL (0.16 ± 0.06), or ΔCt (0.11 ± 0.03). One-way ANOVA, F (2, 6) = 149.5, $p < 0.0001$, Dunnett's multiple comparisons test *versus* WT, KIRBA ΔCCL and ΔCt ****$p < 0.0001$. *G*, PICK1-KIBRA co-cluster density for KIBRA WT (1.00 ± 0.08), ΔCCL (0.10 ± 0.02), or ΔCt (0.09 ± 0.05). Ordinary one-way ANOVA, F (2, 6) = 248.6, $p < 0.0001$, Dunnett's multiple comparisons test *versus* WT, KIRBA ΔCCL and ΔCt ****$p < 0.0001$.

Yeast two-hybrid experiments indicate that KIBRA can dimerize through interactions between the CCL and C2 domains (21), whereas our data demonstrate a clear role for the CCL but not the C2 domain in mediating formation of large KIBRA clusters (Figs. 5, S3, and S4). To identify the modality of KIBRA homodimerization, we transfected HEK293T cells with mGFP-tagged and Myc-tagged KIBRA WT, ΔCCL, ΔC2, ΔCt, or ΔαBR (Fig. 6*C*). Myc-tagged KIBRA was immunoprecipitated using a Myc antibody, and the co-immunoprecipitated mGFP-tagged KIBRA counterpart was detected with a GFP antibody. Quantification of these experiments indicated that no single domain truncation disrupted KIBRA dimerization (Fig. 6*D*). Myc-KIBRA does not interact with GFP alone, indicating that KIBRA homomerization as measured by co-IP is not a nonspecific artifact of KIBRA interaction with protein tags (Fig. S5*B*). These data suggest that KIBRA homodimerization can occur through a multimodal interaction, whereas the presence of both coiled-coil-containing domains is required for higher-order complex formation (Fig. 5).

Discussion

KIBRA in AMPA receptor complexes

KIBRA deletion impairs AMPA receptor trafficking, synaptic plasticity, and memory (14–16). Decreased KIBRA in the brain correlates with tauopathy-related cognitive impairment in humans, and acetylated Tau disrupts KIBRA-mediated AMPA receptor trafficking (28, 29). Conversely, an increased abundance of KIBRA in AMPAR complexes has been shown to enhance hippocampal-dependent learning and memory (50). Despite these findings indicating the importance of KIBRA-dependent signaling in synaptic and brain function, the mechanism by which KIBRA organizes and regulates AMPA receptor complexes has remained elusive. The AMPAR-binding protein PICK1 was previously shown to interact with KIBRA (14), but whether and how PICK1 affected KIBRA-dependent AMPAR regulation was unknown. Here, we show that KIBRA does not interact directly with the AMPAR subunit GluA2 but that PICK1 can mediate complex formation between KIBRA and GluA2. Interestingly, expanding on previous work (17), our data indicate that KIBRA can interact with full-length GluA1, suggesting that there are multiple subunit-specific mechanisms by which KIBRA can form complexes with AMPA receptors (Fig. 7*A*).

Our data, along with others, demonstrate that KIBRA can form a complex with GluA2 *in vivo* (14, 50) and in heterologous cells in a PICK1-dependent manner. However, GluA2 is displaced from PICK1 in large, KIBRA-induced supramolecular clusters, which we hypothesize represent a functionally-distinct PICK1-KIBRA complex (Fig. 7). Intriguingly, recent studies demonstrated that KIBRA promotes Liquid-Liquid Phase Separation (LLPS) to regulate HIPPO pathway signaling (75, 82), and the large KIBRA-PICK1 clusters observed in our study are reminiscent of such LLPS-mediated biomolecular condensates (83), including a critical dependence on KIBRA's coiled-coil domains. LLPS-organized synaptic nanodomains have emerged as mechanisms used to organize synaptic structure and regulate synaptic plasticity (78, 83, 84). Together with our findings, these data raise the intriguing possibility that KIBRA may facilitate synaptic organization, signaling, and plasticity in part through promoting LLPS in excitatory postsynaptic compartments. The spatial organization of tripartite clusters, with KIBRA and PICK1 at the core surrounded by GluA2 (*e.g.* Fig. 2), is reminiscent of LLPS-organized postsynaptic density complexes that have been suggested to segregate different glutamate receptors and their scaffolds into adjacent nanodomains (83). However, while displacement of GluA2 from the PICK1/KIBRA core was consistent across many experiments (Figs. 2, S2, and S4), we saw very few GluA2 ring structures in replicate experiments with lower GluA2 expression (Figs. S2 and S4). As formation of biomolecular condensates is concentration-dependent, future studies in neurons with endogenous protein levels (*e.g.* knock-in of KIBRA coiled-coil domain mutants) will be necessary to determine the physiological impact of KIBRA-mediated LLPS on postsynaptic organization.

GluA2-lacking AMPARs exhibit unique properties, including Ca^{2+} permeability, which play an important role in synaptic plasticity mechanisms and adaptive behavior (35, 85–91). PICK1 has been implicated in subunit-specific trafficking mechanisms that facilitate activity-dependent incorporation of Ca-permeable (CP) AMPARs at synapses (92–94), putatively due to its ability to sequester GluA2-containing AMPARs. In contrast to PICK1 selectivity for interacting with GluA2 (and GluA3) AMPAR subunits, our work indicates that KIBRA can interact with GluA1, suggesting that KIBRA, and PICK1 in complex with KIBRA, may be able to interact with GluA1 homomers. Whether KIBRA plays a role in subunit-specific AMPAR trafficking remains an open question. Identifying the proportion and neuronal localization of KIBRA and PICK1 that function together *versus* in independent complexes will be an important area of investigation for future studies. Furthermore, it is important to note that KIBRA can interact with other AMPAR-binding proteins in addition to PICK1 (17, 50). Thus, the combinatorial composition of AMPAR-binding proteins recruited into KIBRA complexes

H–J, KIBRA WT, ΔCCL or ΔCt were expressed with WT PICK1 in neurons lacking endogenous KIBRA (cultures prepared from KIBRA KO mice). WT KIBRA clusters with PICK1 in mouse hippocampal neurons while KIBRA ΔCCL and ΔCt show diffuse localization and fail to cluster PICK1. *K–M*, quantification of three biological replicates for conditions shown in *H–J*. *K*, KIBRA puncta density for KIBRA WT (1.00 ± 0.22), KIRBA ΔCCL (0.04 ± 0.04), and KIBRA ΔCt (0.02 ± 0.02). Ordinary one-way ANOVA, F (2, 6) = 57.28, $p = 0.0001$, Dunnett's multiple comparisons test vs. WT, KIRBA ΔCCL and ΔCt ***$p = 0.0002$. *L*, PICK1 cluster density when co-expressed with KIBRA WT (1.00 ± 0.27), ΔCCL (0.04 ± 0.04), or ΔCt (0.02 ± 0.04). Ordinary one-way ANOVA, F (2, 6) = 36.35, $p = 0.0004$, Dunnett's multiple comparisons test vs. WT: KIRBA ΔCCL ***$p = 0.0006$, KIBRA ΔCt ***$p = 0.0005$. *M*, PICK1-KIBRA co-cluster density for KIBRA WT (1.00 ± 0.27), ΔCCL (0.02 ± 0.02), or ΔCt (0.02 ± 0.03). Ordinary one-way ANOVA, F (2, 6) = 46.66, $p = 0.0003$, Dunnett's multiple comparisons test *versus* WT, KIRBA ΔCCL and ΔCt ***$p = 0.0004$. Data reported as mean ± SD. Scale bars for *B–D* = 10 μm, and scale bars for *H–J* = 20 μm. For quantification in *E–G* and *K–M*, all values were normalized to the average of the three WT cultures.

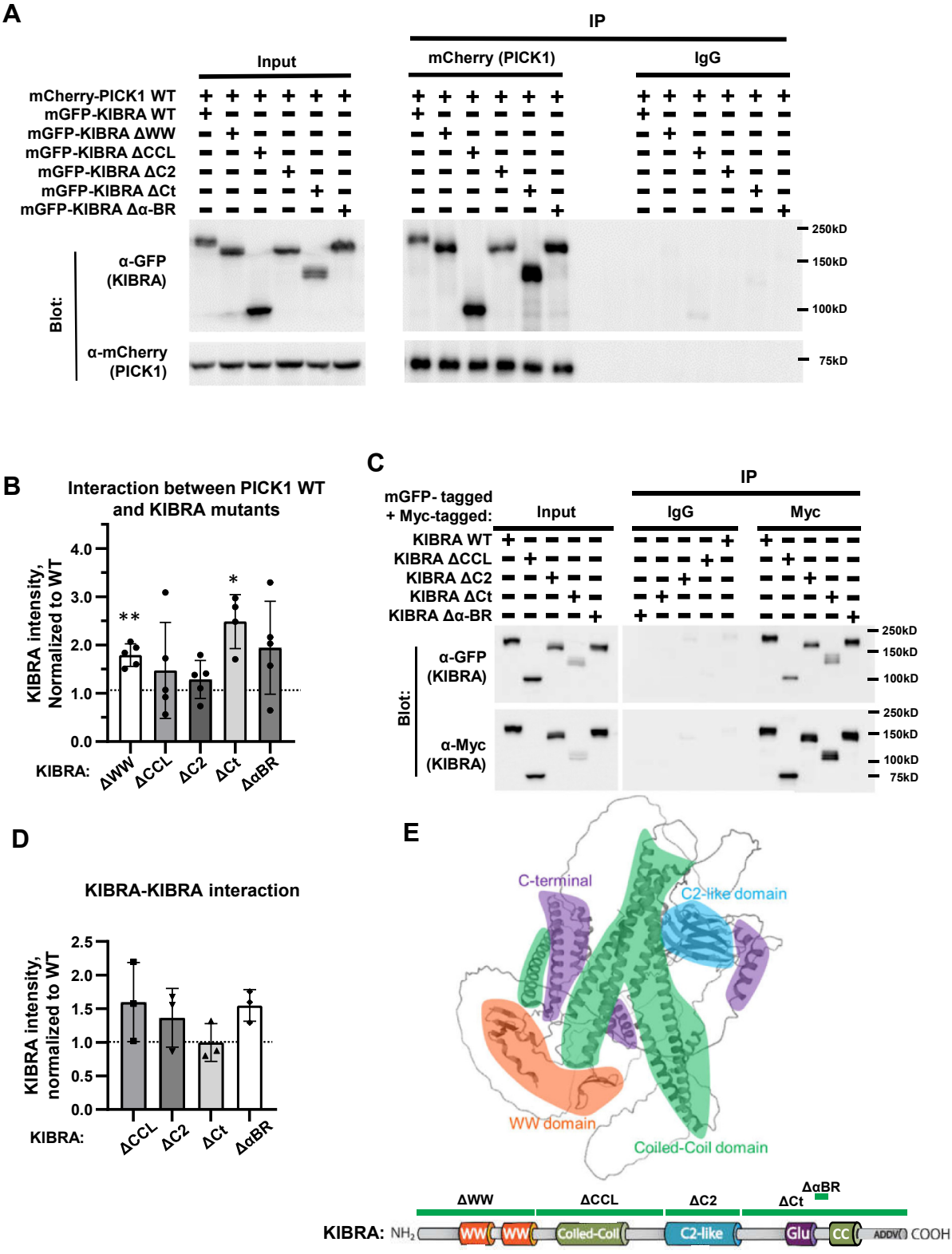

Figure 6. No single domain of KIBRA is essential for interaction between KIBRA and PICK1 or for KIBRA-KIBRA dimerization. *A*, mGFP-KIBRA WT or KIBRA mutants missing the WW domain, coiled-coil linker, C2 domain, C-terminal region, or aPKC binding region (ΔWW, ΔCCL, ΔC2, ΔCt, ΔαBR, respectively) were transfected with mCherry-PICK1 WT into HEK293T cells. Anti-mCherry antibodies were used to immunoprecipitate PICK1, and co-precipitated mGFP-KIBRA variants were detected by immunoblot for GFP. *B*, quantification of five biological replicates under conditions shown in *A*. None of the KIBRA mutants disrupt interaction between KIBRA and PICK1 (values normalized to WT sample from the same blot; ΔCCL 1.48 ± 1.00, p = 0.3465; ΔC2 1.29 ± 0.39, p = 0.1792; ΔαBR 1.94 ± 0.96, p = 0.0936, one-sample t test *versus* 1). KIBRA ΔWW and ΔCt show increased interaction with PICK1 (ΔWW 1.79 ± 0.23, $^{**}p$ = 0.0016; ΔCt 2.49 ± 0.56, $^{*}p$ = 0.0129, one-sample t test *versus* 1). *C*, Myc- and GFP- KIBRA WT, ΔCCL, ΔC2, ΔCt, or ΔαBR were transfected into HEK293T cells. Myc-KIBRA was immunoprecipitated and co-precipitated mGFP-KIBRA was detected by immunoblot. *D*, quantification of three biological replicates

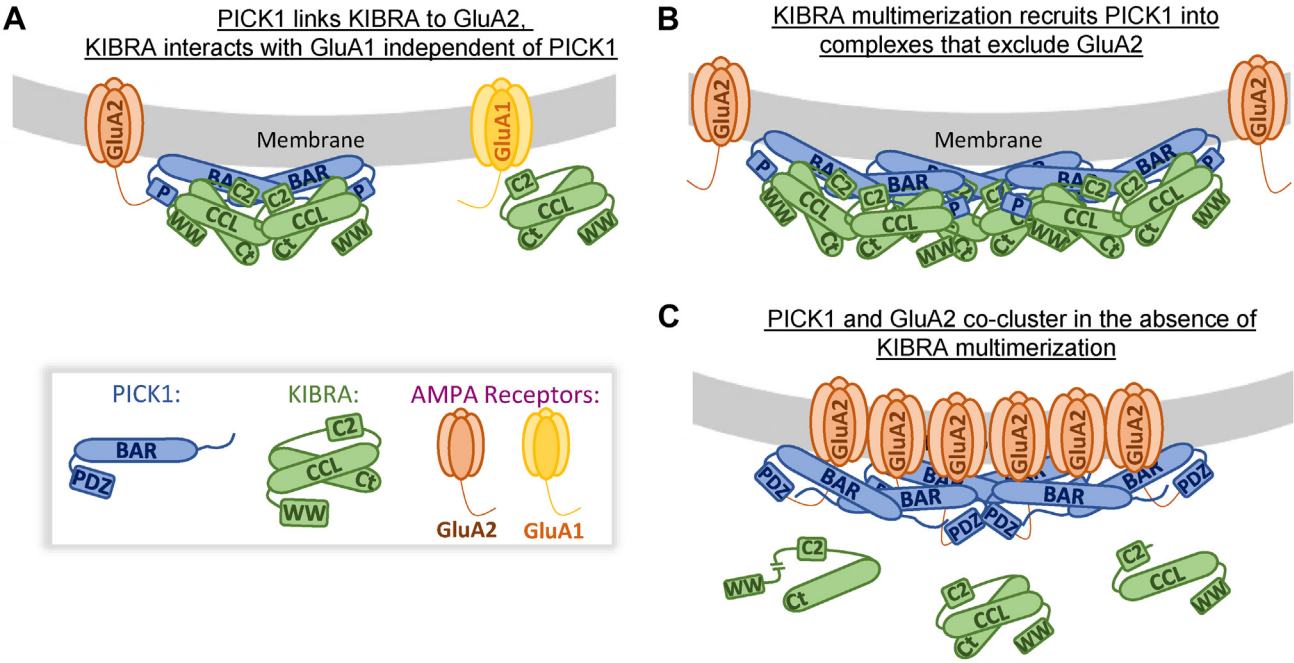

Figure 7. Model of multi-state KIBRA-PICK1-AMPA receptor complexes. *A*, KIBRA can complex with GluA2 indirectly through its interaction with PICK1, whereas KIBRA interacts with GluA1 independent of PICK1. The molecular determinants of KIBRA-GluA1 interaction remain to be identified. The orientation of PICK1 and KIBRA domains shown in the heterotetrameric complex is based on structure predictions using AlphaFold3 (97). *B*, KIBRA multimerization recruits PICK1 into clustered protein assemblies, whereas GluA2 is excluded from the core of KIBRA-PICK1 complexes in this state. *C*, PICK1 and GluA2 co-cluster in the absence of higher-order KIBRA multimerization, highlighted by KIBRA coiled-coil domain mutants that are unable to cluster into multimeric assemblies.

may specify distinct AMPAR regulatory functions; future investigation of activity-dependent and localization-selective changes in the synaptic KIBRA interactome should provide important insight into molecular mechanisms underlying adaptive cognition.

PICK1-KIBRA interaction

KIBRA and PICK1 are multidomain proteins, with each domain serving distinct functions (57, 95). Our data indicate that the PICK1 BAR domain is a major mediator of PICK1-KIBRA interaction, as KIBRA binds to the isolated PICK1 BAR domain and BAR domain point mutants decrease PICK1-KIBRA interaction. Supporting this co-immunoprecipitation data, isolated PICK1 BAR domain is recruited to KIBRA clusters in both HEK293T cells and neurons, whereas BAR domain mutants fail to undergo KIBRA-mediated clustering. Interestingly, mutation of the PICK1 PDZ domain also disrupts PICK1-KIBRA interaction and KIBRA-induced PICK1 clustering. This result could suggest that PICK1 PDZ domain/KIBRA PDZ ligand interactions also contribute to PICK1-KIBRA interaction (96). However, we hypothesize that these data reflect the fact that the PICK1 PDZ and BAR domains can interact, promoting a "closed" conformation of PICK1 that disrupts BAR domain-dependent interactions (57, 59, 62, 63). Binding PDZ ligands promotes an open conformation of PICK1, therefore PICK1 PDZ domain mutation can indirectly inhibit BAR domain-dependent interactions through biasing PICK towards a closed conformation (57, 59, 62). Supporting this interpretation, KIBRA terminates in a type III PDZ ligand, whereas PICK1 preferentially binds type I and II PDZ ligands (52), and our data show that deletion of KIBRA's PDZ ligand does not impair PICK1-KIBRA interaction or co-clustering. BAR domains are a specialized subtype of coiled-coil domain (61, 97). We hypothesize that heterotypic coiled-coil interactions between the PICK1 BAR and KIBRA coiled-coil domains are the primary mediators of PICK1-KIBRA interaction, and that either the coiled-coil linker or C-terminal coiled-coil regions of KIBRA are sufficient for PICK1-KIBRA interaction. Importantly, while our data are consistent with this hypothesis, we did not identify a single domain deletion of KIBRA that disrupted PICK1-KIBRA interaction, thus we cannot rule out other modes of interaction.

PICK1 binds GluA2 through PICK1 PDZ domain/GluA2 PDZ ligand interaction (37, 65). Consistently, we show that BAR domain mutation does not disrupt PICK1-GluA2 interaction, and WT KIBRA does not affect PICK1-GluA2 co-immunoprecipitation. Surprisingly, in the presence of KIBRA, mutation of the PICK1 BAR domain decreases PICK1-GluA2 interaction and PICK1-GluA2 co-clustering. PICK1 5K-E substantially decreases but does not eliminate PICK1-KIBRA interaction. These data suggest that the contact sites or orientation of interaction between KIBRA and PICK1 5K-E

under conditions shown in *C*. No single KIBRA mutant prevents homodimerization (values normalized to WT sample from the same blot; ΔCCL 1.60 ± 0.59, $p = 0.2205$; ΔC2 1.36 ± 0.43, $p = 0.2853$; ΔCt 1.00 ± 0.28, $p = 0.9904$; ΔαBR 1.55 ± 0.23, $p = 0.0560$, one-sample *t* test *versus* 1). *E*, structure and domains of KIBRA. Predicted structure modified from AlphaFold Protein Structure Database. Data reported as mean ± SD.

are altered in a manner that disrupts or occludes PICK1-AMPAR interaction.

KIBRA multimerization

We see that KIBRA forms large clusters when overexpressed in HEK293T cells, in line with previous reports demonstrating that KIBRA promotes LLPS and the formation of large biomolecular condensates to regulate HIPPO signaling in dividing cells (75, 82). Similar to Wang *et al.* (75), we find that deleting the CCL prevents the formation of LLPS-like KIBRA clusters. We further demonstrate that the WW and C2 domains, αBR, and C-terminal PDZ ligand are not required for cluster formation. Our data additionally identify a critical role for the putative coiled-coil region in the KIBRA C-terminus, suggesting that both coiled-coil-containing domains of KIBRA are required for the formation of supramolecular clusters.

Our data confirm previous studies reporting that KIBRA can homodimerize (21, 81); however, we find that no single domain of KIBRA is essential for KIBRA dimerization as assessed by co-immunoprecipitation. Evaluation of KIBRA dimerization using the Yeast-Two-Hybrid system showed that the KIBRA C2 domain can interact with the CCL, and deletion of the entire N-terminus of KIBRA encompassing the WW, CCL, and C2-domains prevented interaction with full-length KIBRA (21). Our data demonstrate that removing just the C2 domain does not impair KIBRA dimerization, suggesting that multiple intermolecular interactions (*e.g.* C2-CCL, heteromeric coiled-coil interactions between the CCL and C-terminal coiled-coil region) are able to support KIBRA dimerization. Notably, KIBRA multimerization, measured by the ability of KIBRA to form large supramolecular clusters, requires both the CCL and C-terminal coiled-coil-containing region, indicating that there are distinct requirements for KIBRA dimerization compared to higher-order multimerization (46). Given the emerging role of biomolecular condensates in organizing synaptic signaling (78, 83, 84), these findings have important implications for understanding the mechanisms by which the human memory and cognitive disorder-associated protein KIBRA regulates synaptic function and plasticity (14–17, 34).

The apparent discrepancy between KIBRA coiled-coil-domains being required for assembly of large KIBRA clusters and subsequent recruitment of PICK1 to these clusters, whereas KIBRA-ΔCCL or KIBRA-ΔCt do not impair KIBRA-KIBRA or KIBRA-PICK1 co-immunoprecipitation may reveal molecular insight into the capacity for multiple functionally-distinct states of KIBRA-organized protein complexes. One possible explanation for this apparent discrepancy is that these protein-protein interactions can be supported by homo- or heterotypic coiled-coil interactions using KIBRA coiled-coil regions in either the CCL or Ct domain. In contrast, KIBRA-dependent formation of large supramolecular complexes requires scaffolding through both domains. Consistent with this idea, KIBRA's CCL and Ct domains are required for inducing LLPS that regulates HIPPO signaling in cultured cells (75, 82). Alternatively, it is possible that the KIBRA-PICK1 clustering observed in heterologous cells reflects an affinity of PICK1 for molecular condensates with the biophysical properties supplied by large KIBRA assemblies, rather than direct interaction between KIBRA and PICK1. It would be informative to test this idea in future studies using a protein capable of inducing LLPS but that does not interact with PICK1. However, our data indicate that relatively conservative point mutants of PICK1 (KD-AA, 5K-E) which decrease PICK1-KIBRA interaction (as measured by co-IP) also prevent PICK1 from co-assembling into KIBRA clusters, suggesting that recruitment of PICK1 to large KIBRA clusters is regulated at least in part by protein interaction as opposed to exclusively through affinity for biomolecular condensates.

In summary, this study reveals molecular mechanisms by which KIBRA can organize key synaptic signaling complexes, with implications for understanding how aberrant KIBRA gene and protein expression impacts memory and disorders of complex cognition (1–13, 18–20).

Experimental procedures

Animal models

The University of Texas Southwestern Medical Center Institutional Animal Care and Use Committees approved all animal protocols in this study. Mice were group housed in a climate-controlled environment on a 12-h light/dark cycle. Food and water were provided *ad libitum*. Generation of KIBRA KO (14) and PICK1 KO (96) mice was described previously. Both lines were maintained on a C57Bl/6N (N10+) background.

cDNA cloning

Mouse KIBRA and PICK1 genes were cloned from mouse tissue by RT-PCR and inserted into pCRII-TOPO (Invitrogen #K4600J10) or pCR-XL-TOPO vectors (Invitrogen #K475010). The genes were moved to a FUGW vector for transient expression or lentivirus generation. The mGFP, mCherry, or Myc tag was inserted at the N-terminus of KIBRA or PICK1. Truncations of KIBRA (delta WW domain, coiled-coil domain, C2 domain, C terminal, and αPKC binding region) or PICK1 (BAR domain) were made with NEBuilder HiFi DNA Assembly Cloning Kit (NEB #E5520S). Mutations of PICK1 (KD-AA and 5K-E) were made with Q5 Site-Directed Mutagenesis Kit (NEB #E0554S). The constructs were purified by NucleoBond Xtra Midi EF (MACHEREY-NAGEL). Myc-GluA1 and Myc-GluA2 were kindly provided by Dr Richard Huganir.

Human embryonic kidney 293T cell culture, transfection, and immunostaining

HEK293T cells (ATCC CRL-3216) were lysed in Trypsin-EDTA (0.25%) (Fisher Scientific # 25-200-072) at 37 °C for 3 min to passage, and cultured in DMEM, high glucose, GlutaMAX Supplement (Life Technologies #10566016) supplied with 10% FBS (Fisher Scientific #26140079), along with 50 U/ml penicillin and 50 μg/ml streptomycin (Penicillin-Streptomycin, Fisher Scientific #15070063). HEK293T cells were transfected by calcium phosphate co-precipitation 36 h after cell passage and collected for biochemical or imaging experiments 36 h after transfection. For immunostaining, cells were

fixed in 4% paraformaldehyde (Sigma-Aldrich #P6148-1KG) plus 4% sucrose (Sigma-Aldrich #S7903-5KG) in PBS at RT (room temperature) for 20 min, permeabilized in 0.2% TritonX-100 in PBS at RT for 10 min, and blocked in 10% NDS (normal donkey serum, Jackson ImmunoResearch #017-000-121) in PBS at RT for 1 h. Cells were then incubated with primary Myc-Tag (9B11) Mouse mAb (Cell Signaling Technology #2276S) in PBS + 3% NDS at RT for 1 h followed by Goat anti Mouse IgG (H+L) Cross-Adsorbed Secondary Antibody (DyLight 405, Fisher Scientific #PI35500) in PBS + 3% NDS at RT for 1 h. After immunostaining, cells were mounted in Fluoroshield histology mounting medium (Sigma-Aldrich #F6182-20ML) and stored at RT until imaging. The authenticity of HEK 293 T cells was not validated using short tandem repeat profiling or other methodology.

Lentivirus production and purification

FUGW mGFP/mCherry-KIBRA (WT, delta coiled-coil domain or C terminal) or PICK1 (WT, 5K-E or BAR domain) was transfected with REV, RRE, and VSV-G into HEK293T cells 36 h after cell passage. Lentivirus was produced form HEK293T cells and released to the supernatant. The supernatant containing the viruses was collected 2 days after transfection and centrifuged at 1000*g* for 5 min at RT to pellet any cell debris. The viral supernatant was concentrated through Amicon Ultra-15 centrifugal filters and stored at −80 °C.

Neonatal mouse hippocampal neuronal culture, transfection, and immunostaining

Hippocampi were dissected from neonatal P0 homozygous KIBRA KO or PICK1 KO mice and incubated with 670 μg/ml Papain (Worthington #LS003119) and 100 μg/ml DNase (Sigma-Aldrich #DN-25) at 37 °C for 10 min. Neurons (2.5×10^5/ml) were plated on poly-L-lysine (Sigma #P2636) coated coverslips in Neurobasal growth medium (Fisher Scientific #21103049) supplemented with 2% B27 (Fisher Scientific #17504044), 2 mM Glutamax (Fisher Scientific #35-050-061), 50 U/ml penicillin, 50 μg/ml streptomycin (Penicillin-Streptomycin, Fisher Scientific #15070063) and 5% Donor Equine Serum (Cytiva #SH30074.03). Three hours after plating, the medium was changed to Neurobasal growth medium supplemented with 2% B27, 2 mM Glutamax, along with 50 U/ml penicillin and 50 μg/ml streptomycin. Neurons were transfected with Lentivirus or NeuroMag Transfection Reagent (OZ Biosciences #KC30800) at DIV10 and observed at DIV14. For immunostaining, neurons were fixed in 4% paraformaldehyde (Sigma-Aldrich #P6148-1KG) plus 4% sucrose (Sigma-Aldrich #S7903-5KG) in PBS at RT (room temperature) for 20 min, permeabilized in 0.2% TritonX-100 in PBS at RT for 10 min, and blocked in 10% NDS (normal donkey serum, Jackson ImmunoResearch #017-000-121) in PBS at RT for 3-4 h. Cells were then incubated with primary Synaptophysin (D8F6H) XP Rabbit mAb (Cell Signaling Technology ##36406) in PBS + 3% NDS at 4 °C overnight followed by Donkey anti-Rabbit IgG (H + L) Highly Cross-Adsorbed Secondary Antibody (Alexa Fluor Plus 405, Fisher Scientific # A48258) in PBS + 3% NDS at RT for 1 h. After immunostaining, cells were mounted in Fluoroshield histology mounting medium (Sigma-Aldrich #F6182-20ML) and stored at RT until imaging.

Co-immunoprecipitation and Western blot

HEK293T cells cultured in 60 mm dishes were lysed in 1 ml PBS with 1% TritonX-100 plus protease inhibitors (cOmplete, Mini Protease Inhibitor Cocktail, Sigma-Aldrich #11836153001) and phosphatase inhibitors (1 mM NaPPi, 5 mM NaF, 1 mM NaVO3). Protein concentration was assayed by Pierce Detergent Compatible Bradford Assay Kit (Thermo Fisher Scientific # 23246). 25 to 50 ul Protein G Magnetic Beads (NEB #S1430S) were incubated with 3 μg GFP (D5.1, Rabbit mAb, Cell Signaling Technology #2956S), mCherry (E5D8F, Rabbit mAb, Cell Signaling Technology #43590S) or Myc (9B11, Mouse mAb, Cell Signaling Technology #2276S) antibody at 4 °C for 1 h. Cell lysate was incubated with antibody-conjugated beads at 4 °C overnight. The incubated beads were washed in 500 μl lysis buffer once, in 500 μl lysis buffer plus 0 to 500 mM NaCl twice and in 500 μl PBS once. The immunoprecipitated proteins were eluted by SDS protein sample buffer (10% glycerol, 62.5 mM Tris/HCl pH 6.8, 2% sodium dodecyl sulfate, 0.01% bromophenol blue, 1.25% beta-mercaptoethanol). Samples were separated *via* SDS-PAGE (8% gels) then transferred to nitrocellulose membrane (LI-COR #926-31092) or PVDF membrane (GE Healthcare #10600023) in cold (∼4 °C) transfer buffer (25 mM Tris, 192 mM glycine, 0.03% sodium dodecyl sulfate and 20% methanol). Membranes were blocked with 2% milk at RT for 1 h and then incubated with primary antibodies (anti-KIBRA kindly provided by Dr Richard Huganir; anti-Flag, Cell Signaling Technology #14793; anti-GFP, mCherry or Myc, Catalog numbers listed above) at 4 °C overnight. Membranes were then washed 5 times with TBST (10 min per wash) followed by incubation with fluorescent secondary antibodies (anti-mouse or anti-rabbit Licor IRDye 680RD or 800CW, #926-68070, 926-68071, 926-32210 or 926-32211) or HRP-conjugated secondary antibodies (Chicken anti Mouse secondary antibody HRP, Fisher Scientific # A15981; Sheep anti Rabbit secondary antibody HRP, Fisher Scientific #A16172; Mouse Anti-rabbit IgG mAb, Cell Signaling Technology #5127) at RT for 1 h, then subjected to a second round of 5× 10 min washes. Membranes incubated with HRP-conjugated secondary antibodies were incubated with Amersham ECL Prime Western Blotting Detection Reagent (GE Healthcare #RPN2232) for 5 min. Fluorescence and Chemiluminescence were imaged using the ChemiDoc MP Imaging System from Bio-Rad, which provides a measure of signal saturation to ensure that no bands are saturated. All Western blots were normalized to input and then to control sample run on the same gel.

Validation of antibody specificity

The anti-GFP antibody (D5.1, Rabbit mAb, Cell Signaling Technology #2956S) was validated by Western blot using lysates from HCC827 cells, either untransfected or transfected

with GFP, as performed by Cell Signaling Technology. The anti-mCherry antibody (E5D8F, Rabbit mAb, Cell Signaling Technology #43590S) was validated by Western blot using lysates from 293T cells, either mock-transfected or transfected with Myc/DDK-tagged mCherry at the C- or N-terminal, as conducted by Cell Signaling Technology. The anti-Myc antibody (9B11, Mouse mAb, Cell Signaling Technology #2276S) was validated by Western blot using lysates from 293T cells, either mock-transfected or transfected with a Myc/DDK-tagged SARS-CoV-2 RNA-dependent RNA polymerase protein. It was also validated by immunofluorescent analysis of COS cells transfected with a Myc-tagged protein, as performed by Cell Signaling Technology. The anti-Flag antibody (D6W5B, Rabbit mAb, Cell Signaling Technology #14793) was validated by Western blot using lysates from 293T cells, either mock-transfected or transfected with Flag-GFP, GFP-Flag, CASQ1-Flag, or FoxG1-Flag, as conducted by Cell Signaling Technology. The anti-synaptophysin antibody (D8F6H, Rabbit mAb, Cell Signaling Technology #36406) was validated by Western blot using lysates from mouse brain (positive control), mouse lung (negative control), and rat brain (positive control). It was also validated by immunofluorescent analysis of mouse retina and brain, as performed by Cell Signaling Technology. The anti-KIBRA antibody was kindly provided by Dr Richard Huganir and validated in our lab by Western blot using lysates from WT and KIBRA KO mouse brain (14, 15).

Confocal imaging and data analysis

All samples were imaged with Zeiss LSM 710 Confocal Microscope at RT. mCherry, mGFP, and immnostained Myc were imaged at 561 nm, 488 nm, and 405 nm excitation, respectively. HEK293T cells were imaged through a 20× dry objective. Neurons were imaged through a 40× oil objective. 3D images were captured at 1 µm intervals as a single optical section. Images were analyzed using ImageJ software. For puncta density analysis, this entailed projecting image Z stacks using the Sum Slices, splitting color channels, subtracting background, and thresholding for each image with the experimenter blind to experimental conditions. Colocalization was determined by overlapping different channels using the Image-Overlay-Add Image function. The number of particles was quantified using the analyze particles function. Analyses in neurons were applied to soma and dendrites, with separate thresholds set to visualize puncta in cell bodies and dendrites. The neuronal area was obtained by manually outlining the neuron and using the measure tool in Image J, and then the total number of puncta in dendrites and soma was divided by the area of the neuron. For line scan analyses a single optical slice was analyzed using the "Plot Profile" function in Image J, determined by the brightest slice in the KIBRA and/or PICK1 channels. The lowest value of the line scan was subtracted from the local background.

Quantification and statistical analysis

Statistical analysis was performed in Graph Pad Prism version 10.3.0. Data are plotted as mean ± SD unless otherwise noted. Detailed information on the statistical test performed for each analysis is noted in the figure legend. $p < 0.05$ was considered significant. Data were quantified from multiple biological replicates representing distinct batches of HEK293T cells (the precise number of replicates is indicated in each figure legend), each containing more than 100 cells, or neuronal cultures prepared from different litters, with neurons from at least two coverslips contributing to each sample. Statistical tests were chosen based on sample size, hypotheses, and agreement with statistical assumptions. Test residuals were examined for normality (D'Agostino-Pearson omnibus, Shapireo-Wilk, and visual inspection of Q-Q plots), and data that showed non-normal residuals were subjected to nonparametric tests, as indicated in the figure legends. Data exclusion: one data point in Figure 6*B* (ΔCt group) was identified as a statistical outlier (ROUT, Q = 1%) and was therefore excluded from the analysis.

Data availability

All data are contained within the article and supporting information.

Supporting information—This article contains supporting information.

Author contributions—X. S. and L. V. writing–review & editing, X. S. and L. V. writing–original draft, X. S. and L. V. visualization, X. S. methodology, X. S. investigation, X. S. and L. V. formal analysis, X. S. and L. V. conceptualization. L. V. supervision; L. V. funding acquisition.

Funding and additional information—National Institutes of Health Grant NIMH 1R01MH117149-01 (L. J. V.). The content is solely the responsibility of the authors and does not necessarily represent the official views of the National Institutes of Health.

Conflict of interest—The authors declare that they have no conflicts of interest with the contents of this article.

Abbreviations—The abbreviations used are: AMPA, α-amino-3-hydroxy-5-methyl-4-isoxazolepropionic acid; BAR, Bin/Amphiphysin/RVS domain; CC, coiled coil; GluA1/GluA2, AMPA receptor subunit 1/2; KIBRA, kidney and brain; LLPS, liquid-liquid phase separation; PICK1, protein interacting with C kinase 1.

References

1. Papassotiropoulos, A., Stephan, D. A., Huentelman, M. J., Hoerndli, F. J., Craig, D. W., Pearson, J. V., *et al.* (2006) Common Kibra alleles are associated with human memory performance. *Science* **314**, 475–478
2. Schaper, K., Kolsch, H., Popp, J., Wagner, M., and Jessen, F. (2008) KIBRA gene variants are associated with episodic memory in healthy elderly. *Neurobiol. Aging* **29**, 1123–1125
3. Preuschhof, C., Heekeren, H. R., Li, S.-C., Sander, T., Lindenberger, U., and Bäckman, L. (2010) KIBRA and CLSTN2 polymorphisms exert interactive effects on human episodic memory. *Neuropsychologia* **48**, 402–408

4. Bates, T. C., Price, J. F., Harris, S. E., Marioni, R. E., Fowkes, F. G. R., Stewart, M. C., *et al.* (2009) Association of KIBRA and memory. *Neurosci. Lett.* **458**, 140–143
5. Almeida, O. P., Schwab, S. G., Lautenschlager, N. T., Morar, B., Greenop, K. R., Flicker, L., *et al.* (2008) KIBRA genetic polymorphism influences episodic memory in later life, but does not increase the risk of mild cognitive impairment. *J. Cell Mol. Med.* **12**, 1672–1676
6. Rovira, E., Mackie, R. S., Clark, N., Squire, P. N., Hendricks, M. D., Pulido, A. M., *et al.* (2016) A role for attention during wilderness navigation: comparing effects of BDNF, KIBRA, and CHRNA4. *Neuropsychology* **30**, 709
7. Vyas, N. S., Ahn, K., Stahl, D. R., Caviston, P., Simic, M., Netherwood, S., *et al.* (2014) Association of KIBRA rs17070145 polymorphism with episodic memory in the early stages of a human neurodevelopmental disorder. *Psychiatry Res.* **220**, 37–43
8. Muse, J., Emery, M., Sambataro, F., Lemaitre, H., Tan, H.-Y., Chen, Q., *et al.* (2014) WWC1 genotype modulates age-related decline in episodic memory function across the adult life span. *Biol. Psychiatry* **75**, 693–700
9. Schuck, N. W., Doeller, C. F., Schjeide, B. M., Schröder, J., Frensch, P. A., Bertram, L., *et al.* (2013) Aging and KIBRA/WWC1 genotype affect spatial memory processes in a virtual navigation task. *Hippocampus* **23**, 919–930
10. Milnik, A., Heck, A., Vogler, C., Heinze, H., de Quervain, D. J., and Papassotiropoulos, A. (2012) Association of KIBRA with episodic and working memory: a meta-analysis. *Am. J. Med. Genet. B: Neuropsychiatr. Genet.* **159**, 958–969
11. Kauppi, K., Nilsson, L.-G., Adolfsson, R., Eriksson, E., and Nyberg, L. (2011) KIBRA polymorphism is related to enhanced memory and elevated hippocampal processing. *J. Neurosci.* **31**, 14218–14222
12. Yasuda, Y., Hashimoto, R., Ohi, K., Fukumoto, M., Takamura, H., Iike, N., *et al.* (2010) Association study of KIBRA gene with memory performance in a Japanese population. *World J. Biol. Psychiatry* **11**, 852–857
13. Vassos, E., Bramon, E., Picchioni, M., Walshe, M., Filbey, F. M., Kravariti, E., *et al.* (2010) Evidence of association of KIBRA genotype with episodic memory in families of psychotic patients and controls. *J. Psychiatr. Res.* **44**, 795–798
14. Makuch, L., Volk, L., Anggono, V., Johnson, R. C., Yu, Y., Duning, K., *et al.* (2011) Regulation of AMPA receptor function by the human memory-associated gene KIBRA. *Neuron* **71**, 1022–1029
15. Mendoza, M. L., Quigley, L. D., Dunham, T., and Volk, L. J. (2022) KIBRA regulates activity-induced AMPA receptor expression and synaptic plasticity in an age-dependent manner. *iScience*. https://doi.org/10.1016/J.ISCI.2022.105623
16. Vogt-Eisele, A., Krüger, C., Duning, K., Weber, D., Spoelgen, R., Pitzer, C., *et al.* (2014) KIBRA (KIdney/BRAin protein) regulates learning and memory and stabilizes Protein kinase Mζ. *J. Neurochem.* **128**, 686
17. Heitz, F. D., Farinelli, M., Mohanna, S., Kahn, M., Duning, K., Frey, M. C., *et al.* (2016) The memory gene KIBRA is a bidirectional regulator of synaptic and structural plasticity in the adult brain. *Neurobiol. Learn Mem.* **135**, 100–114
18. Kos, M. Z., Carless, M. A., Peralta, J., Blackburn, A., Almeida, M., Roalf, D., *et al.* (2016) Exome sequence data from multigenerational families implicate AMPA receptor trafficking in neurocognitive impairment and schizophrenia risk. *Schizophr. Bull.* **42**, 288
19. Parikshak, N. N., Swarup, V., Belgard, T. G., Irimia, M., Ramaswami, G., Gandal, M. J., *et al.* (2016) Genome-wide changes in lncRNA, splicing, and regional gene expression patterns in autism. *Nature* **540**, 423–427
20. Willsey, A. J., Fernandez, T. V., Yu, D., King, R. A., Dietrich, A., Xing, J., *et al.* (2017) *De novo* coding variants are strongly associated with tourette disorder. *Neuron* **94**, 486–499.e9
21. Johannsen, S., Duning, K., Pavenstädt, H., Kremerskothen, J., and Boeckers, T. M. (2008) Temporal-spatial expression and novel biochemical properties of the memory-related protein KIBRA. *Neuroscience* **155**, 1165–1173
22. Hakak, Y., Walker, J. R., Li, C., Wong, W. H., Davis, K. L., Buxbaum, J. D., *et al.* (2001) Genome-wide expression analysis reveals dysregulation of myelination-related genes in chronic schizophrenia. *Proc. Natl. Acad. Sci. U. S. A.* **98**, 4746–4751
23. Hou, L., Bergen, S. E., Akula, N., Song, J., Hultman, C. M., Landén, M., *et al.* (2016) Genome-wide association study of 40,000 individuals identifies two novel loci associated with bipolar disorder. *Hum Mol Genet.* **25**, 3383–3394
24. Voineagu, I., Wang, X., Johnston, P., Lowe, J. K., Tian, Y., Horvath, S., *et al.* (2011) Transcriptomic analysis of autistic brain reveals convergent molecular pathology. *Nature* **474**, 380
25. Fromer, M., Roussos, P., Sieberts, S. K., Johnson, J. S., Kavanagh, D. H., Perumal, T. M., *et al.* (2016) Gene expression elucidates functional impact of polygenic risk for schizophrenia. *Nat. Neurosci. 2016* **19**, 1442–1453
26. Lauriat, T. L., Dracheva, S., Kremerskothen, J., Duning, K., Haroutunian, V., Buxbaum, J. D., *et al.* (2006) Characterization of KIAA0513, a novel signaling molecule that interacts with modulators of neuroplasticity, apoptosis, and the cytoskeleton. *Brain Res.* **1121**, 1–11
27. Nomura, J., Jaaro-Peled, H., Lewis, E., Nuñez-Abades, P., Huppe-Gourgues, F., Cash-Padgett, T., *et al.* (2016) Role for neonatal D-serine signaling: prevention of physiological and behavioral deficits in adult Pick1 knockout mice. *Mol. Psychiatry* **21**, 386–393
28. Tracy, T. E., Sohn, P. D., Minami, S. S., Wang, C., Min, S. W., Li, Y., *et al.* (2016) Acetylated Tau obstructs KIBRA-mediated signaling in synaptic plasticity and promotes tauopathy-related memory loss. *Neuron* **90**, 245–260
29. Kauwe, G., Pareja-Navarro, K. A., Yao, L., Chen, J. H., Wong, I., Saloner, R., *et al.* (2024) KIBRA repairs synaptic plasticity and promotes resilience to tauopathy-related memory loss. *J. Clin. Invest.* **134**. https://doi.org/10.1172/JCI169064
30. Kandel, E. R., Dudai, Y., and Mayford, M. R. (2014) The molecular and systems biology of memory. *Cell* **157**, 163–186
31. Nabavi, S., Fox, R., Proulx, C. D., Lin, J. Y., Tsien, R. Y., and Malinow, R. (2014) Engineering a memory with LTD and LTP. *Nature* **511**, 348
32. Hu, J., Adler, K., Farah, C. A., Hastings, M. H., Sossin, W. S., and Schacher, S. (2017) Cell-specific PKM Isoforms contribute to the maintenance of different forms of persistent long-term synaptic plasticity. *J. Neurosci.* **37**, 2746
33. Ferguson, L., Hu, J., Cai, D., Chen, S., Dunn, T. W., Pearce, K., *et al.* (2019) Isoform specificity of PKMs during long-term facilitation in Aplysia is mediated through stabilization by KIBRA. *J. Neurosci.* **39**, 8632
34. Quigley, L. D., Pendry, R., Mendoza, M. L., Pfeiffer, B. E., and Volk, L. J. (2023) Experience alters hippocampal and cortical network communication *via* a KIBRA-dependent mechanism. *Cell Rep.* **42**, 112662
35. Diering, G. H., and Huganir, R. L. (2018) The AMPA receptor code of synaptic plasticity. *Neuron* **100**, 314–329
36. Shepherd, J. D., and Huganir, R. L. (2007) The cell biology of synaptic plasticity: AMPA receptor trafficking. *Annu. Rev. Cell Dev. Biol.* **23**, 613–643
37. Xia, J., Zhang, X., Staudinger, J., and Huganir, R. L. (1999) Clustering of AMPA receptors by the synaptic PDZ domain-containing protein PICK1. *Neuron* **22**, 179–187
38. Volk, L., Kim, C.-H., Takamiya, K., Yu, Y., and Huganir, R. L. (2010) Developmental regulation of protein interacting with C kinase 1 (PICK1) function in hippocampal synaptic plasticity and learning. *Proc. Natl. Acad. Sci. U. S. A.* **107**, 21784–21789
39. Thorsen, T. S., Madsen, K. L., Rebola, N., Rathje, M., Anggono, V., Bach, A., *et al.* (2010) Identification of a small-molecule inhibitor of the PICK1 PDZ domain that inhibits hippocampal LTP and LTD. *Proc. Natl. Acad. Sci. U. S. A.* **107**, 413–418
40. Kremerskothen, J., Plaas, C., Büther, K., Finger, I., Veltel, S., Matanis, T., *et al.* (2003) Characterization of KIBRA, a novel WW domain-containing protein. *Biochem. Biophys. Res. Commun.* **300**, 862–867
41. Zhang, L., Yang, S., Wennmann, D. O., Chen, Y., Kremerskothen, J., and Dong, J. (2014) KIBRA: in the brain and beyond. *Cell Signal.* **26**, 1392–1399
42. Sudol, M., and Harvey, K. F. (2010) Modularity in the Hippo signaling pathway. *Trends Biochem. Sci.* **35**, 627–633
43. Salah, Z., and Aqeilan, R. I. (2011) WW domain interactions regulate the Hippo tumor suppressor pathway. *Cell Death Dis.* **2**, e172
44. Zheng, Y., and Pan, D. (2019) The hippo signaling pathway in development and disease. *Dev. Cell* **50**, 264–282

45. Strauss, H. M., and Keller, S. (2008) Pharmacological interference with protein-protein interactions mediated by coiled-coil motifs. *Handb. Exp. Pharmacol.* **186**, 461–482
46. Ciani, B., Bjelić, S., Honnappa, S., Jawhari, H., Jaussi, R., Payapilly, A., *et al.* (2010) Molecular basis of coiled-coil oligomerization-state specificity. *Proc. Natl. Acad. Sci. U. S. A.* **107**, 19850–19855
47. Posner, M. G., Upadhyay, A., Ishima, R., Kalli, A. C., Harris, G., Kremerskothen, J., *et al.* (2018) Distinctive phosphoinositide- and Ca2+-binding properties of normal and cognitive performance–linked variant forms of KIBRA C2 domain. *J. Biol. Chem.* **293**, 9335
48. Duning, K., Schurek, E. M., Schlüter, M., Bayer, M., Reinhardt, H. C., Schwab, A., *et al.* (2008) KIBRA modulates directional migration of podocytes. *J. Am. Soc. Nephrol.* **19**, 1891–1903
49. Harris, B. Z., and Lim, W. A. (2001) Mechanism and role of PDZ domains in signaling complex assembly. *J Cell Sci.* **114**, 3219–3231
50. Stepan, J., Heinz, D. E., Dethloff, F., Bajaj, T., Zellner, A., Hafner, K., *et al.* (2022) Hippo-released WWC1 facilitates AMPA receptor regulatory complexes for hippocampal learning. *Cell Rep.* **41**, 111766
51. Stepan, J., Heinz, D. E., Dethloff, F., Wiechmann, S., Martinelli, S., Hafner, K., *et al.* (2024) Inhibiting Hippo pathway kinases releases WWC1 to promote AMPAR-dependent synaptic plasticity and long-term memory in mice. *Sci. Signal.* **17**, eadj6603
52. Xu, J., and Xia, J. (2007) Structure and function of PICK1. *Neurosignals* **15**, 190–201
53. Herlo, R., Lund, V. K., Lycas, M. D., Jansen, A. M., Khelashvili, G., Andersen, R. C., *et al.* (2018) An amphipathic helix directs cellular membrane curvature sensing and function of the BAR domain protein PICK1. *Cell Rep.* **23**, 2056–2069
54. Madsen, K. L., Beuming, T., Niv, M. Y., Chang, C. W., Dev, K. K., Weinstein, H., *et al.* (2005) Molecular determinants for the complex binding specificity of the PDZ domain in PICK1. *J. Biol. Chem.* **280**, 20539–20548
55. Jin, W., Ge, W. P., Xu, J., Cao, M., Peng, L., Yung, W., *et al.* (2006) Lipid binding regulates synaptic targeting of PICK1, AMPA receptor trafficking, and synaptic plasticity. *J. Neurosci.* **26**, 2380–2390
56. Citri, A., and Malenka, R. C. (2008) Synaptic plasticity: multiple forms, functions, and mechanisms. *Neuropsychopharmacology* **33**, 18–41
57. Hanley, J. G. (2008) PICK1: a multi-talented modulator of AMPA receptor trafficking. *Pharmacol. Ther.* **118**, 152–160
58. Cao, M., Xu, J., Shen, C., Kam, C., Huganir, R. L., and Xia, J. (2007) PICK1-ICA69 heteromeric BAR domain complex regulates synaptic targeting and surface expression of AMPA receptors. *J. Neurosci.* **27**, 12945–12956
59. Lu, W., and Ziff, E. B. (2005) PICK1 interacts with ABP/GRIP to regulate AMPA receptor trafficking. *Neuron* **47**, 407–421
60. Hanley, J. G., Khatri, L., Hanson, P. I., and Ziff, E. B. (2002) NSF ATPase and α-/β-SNAPs disassemble the AMPA receptor-PICK1 complex. *Neuron* **34**, 53–67
61. Ren, G., Vajjhala, P., Lee, J. S., Winsor, B., and Munn, A. L. (2006) The BAR domain proteins: molding membranes in fission, fusion, and phagy. *Microbiol. Mol. Biol. Rev.* **70**, 37–120
62. Rocca, D. L., Martin, S., Jenkins, E. L., and Hanley, J. G. (2008) Inhibition of Arp2/3-mediated actin polymerisation by PICK1 regulates neuronal morphology and AMPA receptor endocytosis. *Nat. Cell Biol.* **10**, 259
63. He, Y., Liwo, A., Weinstein, H., and Scheraga, H. A. (2011) PDZ binding to the BAR domain of PICK1 is elucidated by coarse-grained molecular dynamics. *J. Mol. Biol.* **405**, 298–314
64. Madsen, K. L., Eriksen, J., Milan-Lobo, L., Han, D. S., Niv, M. Y., Ammendrup-Johnsen, I., *et al.* (2008) Membrane localization is critical for activation of the PICK1 BAR domain. *Traffic* **9**, 1327–1343
65. Dev, K. K., Nishimune, A., Henley, J. M., and Nakanishi, S. (1999) The protein kinase Cα binding protein PICK1 interacts with short but not long form alternative splice variants of AMPA receptor subunits. *Neuropharmacology* **38**, 635–644
66. Jaafari, N., Henley, J. M., and Hanley, J. G. (2012) PICK1 mediates transient synaptic expression of GluA2-lacking AMPA receptors during glycine-induced AMPA receptor trafficking. *J. Neurosci.* **32**, 11618–11630
67. Anggono, V., Koç-Schmitz, Y., Widagdo, J., Kormann, J., Quan, A., Chen, C. M., *et al.* (2013) PICK1 interacts with PACSIN to regulate AMPA receptor internalization and cerebellar long-term depression. *Proc. Natl. Acad. Sci. U. S. A.* **110**, 13976–13981
68. Anggono, V., and Huganir, R. L. (2012) Regulation of AMPA receptor trafficking and synaptic plasticity. *Curr. Opin. Neurobiol.* **22**, 461–469
69. He, J., Xia, M., Yeung, P. K. K., Li, J., Li, Z., Chung, K. K., *et al.* (2018) PICK1 inhibits the E3 ubiquitin ligase activity of Parkin and reduces its neuronal protective effect. *Proc. Natl. Acad. Sci. U. S. A.* **115**, E7193–E7201
70. Fujii, K., Maeda, K., Hikida, T., Mustafa, A. K., Balkissoon, R., Xia, J., *et al.* (2006) Serine racemase binds to PICK1: potential relevance to schizophrenia. *Mol. Psychiatry* **11**, 150–157
71. Williams, M. E., Wu, S. C. Y., McKenna, W. L., and Hinck, L. (2003) Surface expression of the netrin receptor UNC5H1 is regulated through a protein kinase C-interacting protein/protein kinase-dependent mechanism. *J. Neurosci.* **23**, 11279–11288
72. El Far, O., Airas, J., Wischmeyer, E., Nehring, R. B., Karschin, A., and Betz, H. (2000) Interaction of the C-terminal tail region of the metabotropic glutamate receptor 7 with the protein kinase C substrate PICK1. *Eur. J. Neurosci.* **12**, 4215–4221
73. Duggan, A., García-Añ overos, J., and Corey, D. P. (2002) The PDZ domain protein PICK1 and the sodium channel BNaC1 interact and localize at mechanosensory terminals of dorsal root ganglion neurons and dendrites of central neurons. *J. Biol. Chem.* **277**, 5203–5208
74. Staudinger, J., Lu, J., and Olson, E. N. (1997) Specific interaction of the PDZ domain protein PICK1 with the COOH terminus of protein kinase C-α. *J. Biol. Chem.* **272**, 32019–32024
75. Wang, L., Choi, K., Su, T., Li, B., Wu, X., Zhang, R., *et al.* (2022) Multiphase coalescence mediates Hippo pathway activation. *Cell* **185**, 4376–4393.e18
76. Höhne, M., Lorscheider, J., von Bardeleben, A., Dufner, M., Scharf, M. A., Gödel, M., *et al.* (2011) The BAR domain protein PICK1 regulates cell recognition and morphogenesis by interacting with neph proteins. *Mol. Cell Biol.* **31**, 3241
77. Sathe, M., Muthukrishnan, G., Rae, J., Disanza, A., Thattai, M., Scita, G., *et al.* (2018) Small GTPases and BAR domain proteins regulate branched actin polymerisation for clathrin and dynamin-independent endocytosis. *Nat. Commun.* **9**, 1835
78. Zeng, M., Shang, Y., Araki, Y., Guo, T., Huganir, R. L., and Zhang, M. (2016) Phase transition in postsynaptic densities underlies formation of synaptic complexes and synaptic plasticity. *Cell* **166**, 1163–1175.e12
79. Xiao, B., Tu, J. C., Petralia, R. S., Yuan, J. P., Doan, A., Breder, C. D., *et al.* (1998) Homer regulates the association of group 1 metabotropic glutamate receptors with multivalent complexes of homer-related, synaptic proteins. *Neuron* **21**, 707–716
80. Hayashi, M. K., Tang, C., Verpelli, C., Narayanan, R., Stearns, M. H., Xu, R. M., *et al.* (2009) The postsynaptic density proteins Homer and Shank form a polymeric network structure. *Cell* **137**, 159–171
81. Wennmann, D. O., Schmitz, J., Wehr, M. C., Krahn, M. P., Koschmal, N., Gromnitza, S., *et al.* (2014) Evolutionary and molecular facts link the WWC protein family to hippo signaling. *Mol. Biol. Evol.* **31**, 1710–1723
82. Bonello, T. T., Cai, D., Fletcher, G. C., Wiengartner, K., Pengilly, V., Lange, K. S., *et al.* (2023) Phase separation of Hippo signalling complexes. *EMBO J.* **42**, e112863
83. Hosokawa, T., Liu, P. W., Cai, Q., Ferreira, J. S., Levet, F., Butler, C., *et al.* (2021) CaMKII activation persistently segregates postsynaptic proteins *via* liquid phase separation. *Nat. Neurosci.* **24**, 777–785
84. Zeng, M., Chen, X., Guan, D., Xu, J., Wu, H., Tong, P., *et al.* (2018) Reconstituted postsynaptic density as a molecular platform for understanding synapse formation and plasticity. *Cell* **174**, 1172–1187.e16
85. Clem, R. L., and Huganir, R. L. (2010) Calcium-permeable AMPA receptor dynamics mediate fear memory erasure. *Science* **330**, 1108–1112

86. Clem, R. L., Anggono, V., and Huganir, R. L. (2010) PICK1 regulates incorporation of calcium-permeable AMPA receptors during cortical synaptic strengthening. *J. Neurosci.* **30**, 6360–6366
87. Plant, K., Pelkey, K. A., Bortolotto, Z. A., Morita, D., Terashima, A., McBain, C. J., *et al.* (2006) Transient incorporation of native GluR2-lacking AMPA receptors during hippocampal long-term potentiation. *Nat. Neurosci.* **9**, 602–604
88. Soares, C., Lee, K. F. H., Nassrallah, W., and Béïque, J. C. (2013) Differential subcellular targeting of glutamate receptor subtypes during homeostatic synaptic plasticity. *J Neurosci.* **33**, 13547–13559
89. Kim, S., and Ziff, E. B. (2014) Calcineurin mediates synaptic scaling *via* synaptic trafficking of Ca2+-permeable AMPA receptors. *PLoS Biol.* **12**, e1001900
90. Sanderson, J. L., Gorski, J. A., and Dell'Acqua, M. L. (2016) NMDA receptor-dependent LTD requires transient synaptic incorporation of Ca^{2+}-permeable AMPARs mediated by AKAP150-anchored PKA and calcineurin. *Neuron* **89**, 1000–1015
91. McCutcheon, J. E., Wang, X., Tseng, K. Y., Wolf, M. E., and Marinelli, M. (2011) Calcium-permeable AMPA receptors are present in nucleus accumbens synapses after prolonged withdrawal from cocaine self-administration but not experimenter-administered cocaine. *J. Neurosci.* **31**, 5737–5743
92. Schneider, A., Huentelman, M. J., Kremerskothen, J., Duning, K., Spoelgen, R., and Nikolich, K. (2010) KIBRA: a new gateway to learning and memory? *Front. Aging Neurosci.* **2**, 1232
93. Cao, R., Zhu, R., Sha, Z., Qi, S., Zhong, Z., Zheng, F., *et al.* (2023) WWC1/2 regulate spinogenesis and cognition in mice by stabilizing AMOT. *Cell Death Dis.* **14**, 491
94. Habermann, B. (2004) The BAR-domain family of proteins: a case of bending and binding? *EMBO Rep.* **5**, 250–255
95. Hsu, R., Woodroffe, A., Lai, W.-S., Cook, M. N., Mukai, J., Dunning, J. P., *et al.* (2007) Nogo Receptor 1 (RTN4R) as a candidate gene for schizophrenia: analysis using human and mouse genetic approaches. *PLoS One* **2**, e1234
96. Gardner, S. M., Takamiya, K., Xia, J., Suh, J. G., Johnson, R., Yu, S., *et al.* (2005) Calcium-permeable AMPA receptor plasticity is mediated by subunit-specific interactions with PICK1 and NSF. *Neuron* **45**, 903–915
97. Abramson, J., Adler, J., Dunger, J., Evans, R., Green, T., Pritzel, A., *et al.* (2024) Accurate structure prediction of biomolecular interactions with AlphaFold 3. *Nature* **630**, 493–500